The effects of serotonin deficiency in mice: Focus on the GABAergic system

Doctoral thesis for a doctoral degree
at the Graduate School of Life Sciences,
Julius-Maximilians-Universität Würzburg,
Section Neuroscience

Submitted by

Jonas Waider

From
Kirchheimbolanden

Würzburg, 2012

Submitted on: 11.07.2012

Members of the doctorate committee:

Chairperson:	Professor Dr. Peter Jakob
Primary Supervisor:	Professor Dr. Klaus-Peter Lesch
Supervisor (Second):	Professor Dr. Bertram Gerber
Supervisor (Third):	Professor Turhan Canli, Ph.D

Date of Public Defense: ……..…….

Date of receipt of Certificates: ……

Table of contents

1 Introduction

1.1 Serotonin - discovery and function

Serotonin (5-hydroxytryptamine, 5-HT) was discovered in 1933. At this time a compound out of intestinal mucosa with the ability to contract smooth muscles, called enteramine was found (Erspamer and Vialli, 1937) and later renamed into 5-HT (Erspamer and Asero, 1952). 95% of the body's 5-HT is found in peripheral organs like the gastrointestinal tract regulating its motility, thrombocytes of the blood system inducing blood clotting and vasoconstriction and the pineal gland as a precursor of melatonin involved in the regulation of circadian rhythms. Only 5% of the bodies 5-HT resides within the central nervous system (CNS) playing an important role as emotional regulator (Berger et al., 2009).

5-HT is synthesized from the amino acid L-tryptophan (Trp). In the rate limiting step tryptophan hydroxylase (TPH) hydroxylates Trp into 5-OH Trp, which is decarboxylated in the following step into 5-HT. 5-HT acts through more than fifteen different 5-HT receptors, classified into seven families (Bockaert et al., 2006) located on the pre- and postsynapse. All 5-HT receptors instead of the 5-HT3 receptors, which are the only ionotropic receptors, are metabotropic receptors coupled to a G-protein dependent second messenger system.

5-HT signaling at the synapse is terminated by reuptake of 5-HT into the presynapse by the 5-HT transporter (5-HTT) and either restored into synaptic vesicle via the vesicular monoamine transporter (VMAT2) or degraded by monoamine oxidase (MAO) into 5-hydroxy indole acetic acid (5-HIAA) (Fig 1-1).

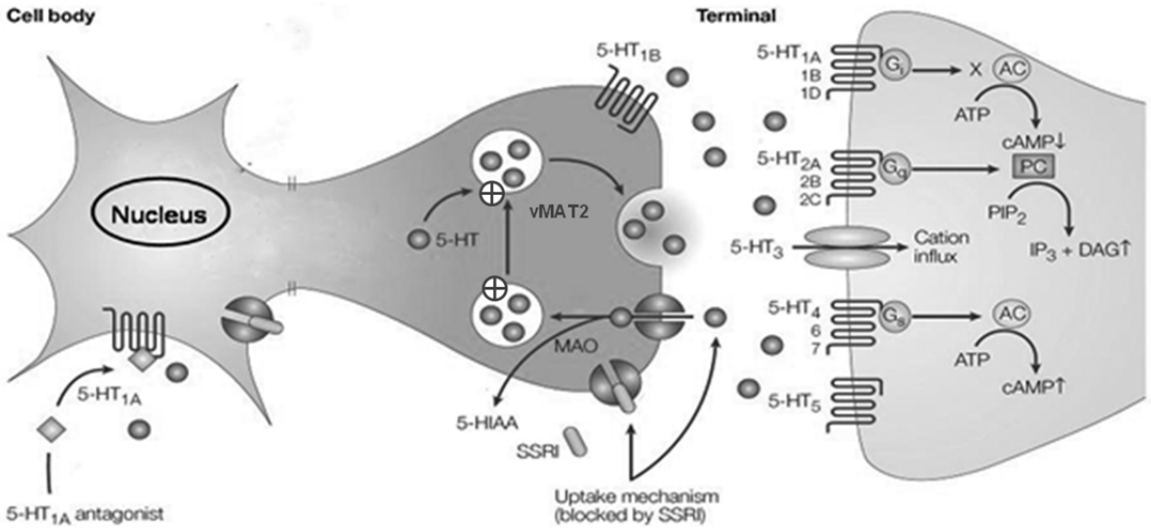

Fig.1-1 Serotonergic neurotransmission (Adapted from Wong *et al., 2005*)
5-HT activates different 5-HT receptor subtypes classified into 7 families. The action of 5-HT is terminated by its fast reuptake into the presynapse via the 5-HT transporter. Selective 5-HT reuptake inhibitors (SSRIs) and tricyclic antidepressants block the 5-HT transporter leading to an increased concentration of 5-HT in the synaptic cleft. After reuptake into the presynaptic 5-HT terminals, 5-HT is either taken up by storage vesicles for a further release or degraded by monoamine oxidase (MAO). 5-HIAA: 5-Hydroxyindolacetic acid; AC: adenylate cyclase; DAG: diacylglycerol; IP3: inositol-1, 4, 5-trisphosphate; PIP2: phosphatidylinositol-4, 5-bisphosphate; cAMP: 3-5-cyclic adenosine monophosphate; ATP: adenosine-5-triphosphate

1.2 TPH2 in disorders of cognitive control and emotion regulation

Besides its peripheral function, 5-HT is involved in the regulation of mood and the development of the central nervous system. Thus alterations in 5-HT function are implicated in the pathophysiology of a wide spectrum of neuropsychiatric disorders, including depression (Zill et al., 2004, Van Den Bogaert et al., 2006, Haghighi et al., 2008), anxiety (Canli and Lesch, 2007, Canli et al., 2008), obsessive-compulsive disorders (OCD), bipolar disorder (Harvey et al., 2004, Lopez et al., 2007, Cichon et al., 2008), schizophrenia, autism and attention-deficit/hyperactivity disorder (ADHD) (Lesch, 2004, Jacob et al., 2005, Canli and Lesch, 2007).

Human variants with single nucleotide polymorphisms (SNPs) within the transcriptional control region of *TPH2* have been associated with reduced functionality of *TPH2* (Zhang et al., 2004, Chen et al., 2008). In addition personality and behavioral traits (Gutknecht et al., 2007) as well as clinical cohorts characterized by emotional dysregulation such as OCD (Mossner et al., 2006) and ADHD (Walitza et al., 2005, Baehne et al., 2009, Lesch, 2011) could be associated with functional SNP's in the *Tph2* gene, which biased the responsiveness of the amygdala to emotional faces (Brown et al., 2005, Canli et al., 2005). Thus, alterations of 5-HT synthesis in disorders of emotion regulation seem to be mediated by *TPH2* activity (Table 1).

Table 1 Summary of polymorphisms of *TPH2* associated with common psychiatric disorders and their endophenotypes.

TPH2 polymorphisms	Association	Reference
rs4570625; rs11178997; rs4565946	Childhood ADHD	Walitza et al., 2005
rs4570625; rs4565946	Preferential transmission of a haplotype of *TPH2* in early-onset OCD	Mössner et al., 2006
rs11178997; rs4570625	Functionality of *TPH2* promoter polymorphisms in serotonergic cell culture	Scheuch et al., 2007
rs4570625; rs11178997473; rs11178998	Functionality of *TPH2* promoter polymorphisms in serotonergic cell culture	Chen et al., 2008
rs33849125	Loss of function of *TPH2* in PC12 cells	Zhang et al., 2005
rs4570625	Responsiveness of the amygdala in a face-processing task	Brown et al., 2005
rs4570625	Responsiveness of the amygdala in a face-processing task	Canli et al., 2005

rs4570625	Additional effects of *TPH2* and 5-HTT genotype on amygdala function and affective processing	Canli et al., 2008
rs4570625; rs11178997	Altered function of the prefrontal cortex during a response inhibition task in adult patient with ADHD	Baehne et al., 2009

1.3 Development and anatomy of the serotonergic system

5-HT positive neurons appear in the anterior murine embryonic hindbrain around embryonic day (E) 10.5 (Pattyn et al., 2004) derived from ventral neuroepethelial progenitor cells within rostral and caudal cell clusters (Cordes, 2005) (Fig.1-2). The rostral subdivision forms the caudal linear nucleus (CLi), the dorsal raphe nucleus (DR: B6, B7) and the median raphe nucleus (MnR: B9, B8 and B5). These serotonergic neurons send distinct projections into structures of the forebrain regions regulating perception, cognition and emotional states (Hornung, 2003). The caudal cluster, which projects mainly to the spinal cord and cerebellum, consists of the raphe pallidus nucleus (B1), the raphe obscurus nucleus (B2) and the raphe magnus nucleus (B3). This subsystem is involved in motor activity, pain control, and regulation of the autonomic nervous system (Azmitia and Whitaker-Azmitia, 1991, Hornung, 2003), (Berger et al., 2009). Serotonergic differentiation is induced by a complex cascade of transcription factors in the notochord and floor plate of the embryo (Fig.1-2). Induced by sonic hedgehog (Shh) the cascade of the transcription factors finally leads to expression of *Lmx1b* and *Pet-1*. These two factors act in concert to activate expression of 5HT-specific genes and give rise to the final serotonergic phenotype. Mice deficient in *Pet-1* are characterized by developmental loss of up to 80%, whereas *Lmx1b* deficient mice loose all 5-HT neurons until adulthood. Therefore, expression of these two factors is thought to be

necessary for specification of most serotonergic precursor cells into mature neurons and for their maintenance (Dai et al., 2008, Liu et al., 2010). However, other unknown factors might act in concert with the known transcription factors to specify development of different raphe cell groups.

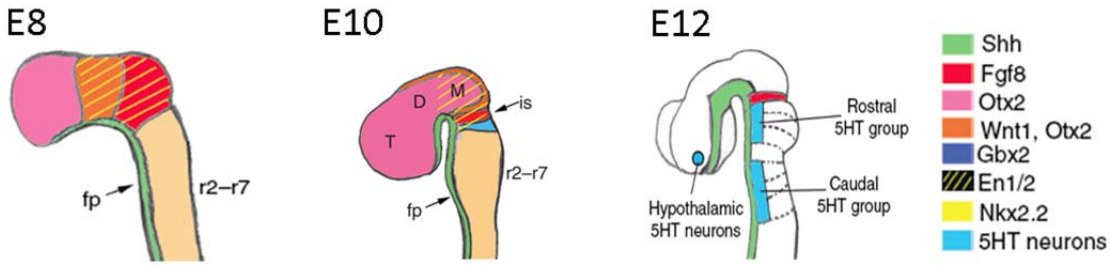

Fig.1-2 Development of serotonergic neurons (Adapted from Cordes, 2005)
Between embryonic day (E) 8 and E12, a rostral and a caudal group of serotonergic (5-HT) neurons are born in the murine embryonic hindbrain dependent on the expression of specific factors. Shh: Sonic hedgehog; Fgf8: Fibroblast growth factor 8; En1/2: engrailed 1/2

In line with the distinct action of transcription factors, the morphology of 5-HT neurons differs between the ascending raphe nuclei. Serotonergic neurons from the MnR and DR nucleus densely innervate the prefrontal cortex. Furthermore, the DR projects most heavily into the striatum, while the MR predominantly innervates septum and dorsal hippocampus The amygdala is innervated by the DR neurons as well as the ventral hippocampus (Molliver, 1987). In addition to their target specificity, axons emanating from the DR form thick fiber tracts with short thin branches and large non-fusiform buttons, whereas MnR neurons possess thin axons with small fusiform buttons. Besides their distinct morphology (Fig.1-3), fine serotonergic fibers from the DR seem to express 5-HTT. In contrast, MR axons seem to lack 5-HTT expression (Brown and Molliver, 2000). Thus these two distinct serotonergic systems

maybe differentially modulated by drugs that block 5-HT reuptake (e.g. SSRIs) and may elicit a differential role in the treatment of affective disorders (Hensler, 2006).

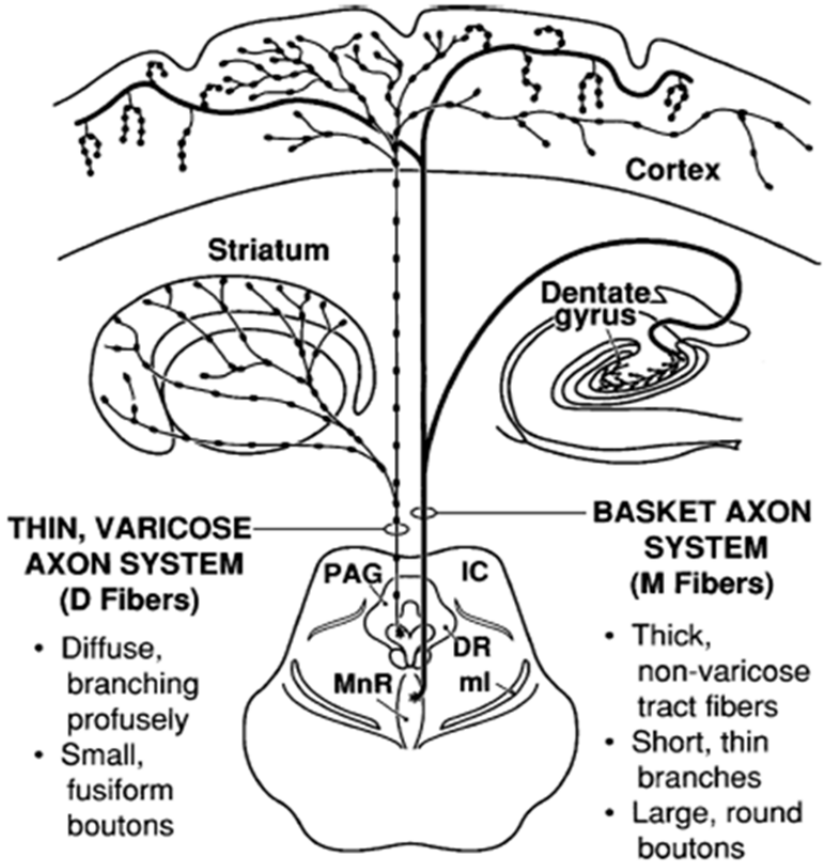

Fig.1-3 Different serotonergic fibers innervating limbic structures (Hensler, 2006)

1.4 Murine models of serotonergic function

Murine models of serotonergic deficiency greatly enhanced our understanding of the serotonergic system. 5-HTT$^{-/-}$ mice characterized by increased extracellular 5-HT levels (Kim et al., 2005) show a more anxious (Holmes et al., 2003) and less aggressive phenotype (Holmes et al., 2002). Monoamine oxidase A (MAO A) deficient mice, which lack the main 5-HT degrading enzyme, display in a more aggressive behavior (Cases et al., 1995). Inactivation of these two important proteins in 5-HT homeostasis cause severe abnormalities in the development of thalamocortical and retinal axons (Gaspar et al., 2003). Furthermore,

mice with a non-functional 5-HT1A receptor display heightened anxiety-like behavior. Rescue of the 5-HT1A receptor function in the hippocampus and cortex during the early postnatal period has been shown to be sufficient for a normal anxiety phenotype (Gross et al, 2002), which implicates that anxiety-like behavior depends on serotonergic signaling within the cortex during critical periods. *Pet-1* deficient mice with an 80% reduction in 5-HT levels and 5-HT positive cells in the CNS were associated with heightened anxiety- and aggressive-like behavior (Hendricks et al., 2003). In another study, these mice showed decreased levels of anxiety in exploratory behavior, but enhanced freezing in fear conditioning tests. This is probably due to the distinct connectivity of remaining 5-HT neurons in relation to alterations in specific targeted nuclei, which are likely to account for the altered anxiety-like behavior (Kiyasova et al., 2011). Constitutive $Lmx1b^{-/-}$ mice lack central serotonergic neurons but show perinatal lethality; whereas conditional $Lmx1b^{-/-}$ mice survive without apparent developmental abnormalities (Zhao et al., 2006), which points to a lethal effect of 5-HT neuron loss. Furthermore, in a triple transgenic mouse model, the expression of tetanus toxin (Tox) gene is directed to all *Pet-1* expressing 5-HT neurons resulting in a complete loss of 5-HT vesicle release. The reduced anxiety but enhanced prepulse-mediated inhibition of the acoustic startle reflex in these mice is indicative of enhanced sensory gating and enhanced conditioned contextual fear response. Furthermore, it was found that suppression of 5-HT synaptic release restricted to those neurons in the rostral clusters that innervate forebrain areas block the anxiolytic-like behavioral response, whereas fear and prepulse inhibition responses remain unchanged (Kim et al., 2009)

1.5 Serotonin and GABA in limbic brain structures

Serotonergic axons densely innervate the prefrontal cortex (PFC) (Di Pino et al., 2004), hippocampus (Gulyas et al., 1999) and amygdala (Sadikot and Parent, 1990), which constitute interconnected limbic brain circuits involved in emotion regulation.

The basolateral complex of the amygdala (BLC) is a structure fundamentally involved in the regulation of fear and anxiety (Pape and Pare, 2010) and is densely innervated by serotonergic fibers from the dorsal raphe nucleus (Molliver, 1987). Within the BLC of rats, PV neurons represent a subgroup of GABAergic neurons (McDonald and Mascagni, 2001). They specifically express 5-HT2A receptors (McDonald and Mascagni, 2007, Bombardi, 2011) and tightly control glutamatergic output neurons by perisomatic inhibition (Muller et al., 2005, Holmes, 2008), whereas 5-HT2C receptors are expressed on other interneuron subtypes (Wright et al., 1995, Bonn et al., 2012). Furthermore, anxiogenic compounds have been shown to recruit GABAergic neurons including the PV subpopulation in the BLC most likely via serotonergic input from the dorsal raphe nucleus (Hale et al., 2010)

The dorsal hippocampus was shown to be critically involved in context-dependent learning processes (Chowdhury et al., 2005, Fendt et al., 2005, Quinn et al., 2008) with the dorsal and ventral hippocampus as interconnected but functionally separate subdivisions integrated in different neuronal networks, thus mediating different behaviors (Fanselow and Dong, 2010). Furthermore, the distribution of different interneuron subtypes including the PV-specific population was shown to be distinct for both subregions of the hippocampus (Jinno and Kosaka, 2010).

The GABAergic system is implicated in the pathogenesis of anxiety and mood disorders (Lydiard, 2003). Several in vitro and in vivo studies showed a morphogenic effect of 5-HT on migration, differentiation and survival of GABAergic interneurons (Gaspar et al., 2003, Di Pino et al., 2004, Bonnin et al., 2007). Furthermore, 5-HT influences cortical GABAergic cell migration via 5-HT6 receptors during late embryonic stages (Riccio et al., 2009), thus assisting their integration into cortical networks (Vitalis et al., 2007).

The dual role hypothesis for 5-HT by Graeff and Dakin (Graeff et al., 1996) claims that DR neurons are activated in threatening situations of proximal or distal danger inhibiting amygdala neurons through 5-HT2A and 5-HT2C receptors, whereas inhibiting neurons in the dorsal periaqueductal gray (PAG) responsible for the flight response (see Fig 1-4).

On the other hand, persistent and uncontrollable chronic stress activates MnR neurons, which will inhibit the dorsal hippocampus. MRN projections to the dorsal hippocampus might be involved to disassociate previously learned negative associations (Solomon et al., 1980) and thus enable a disconnection of aversive cues with their emotional consequences after repeated experience (Deakin and Graeff, 1991). This resilience mechanism to chronic stress may be mediated probably through 5-HT1A heteroreceptors in the dorsal hippocampus. Holmes (2008) further elaborated on this hypothesis to explain the role of the DR nucleus in the modulation of fear and anxiety. Different functioning of distinct 5-HT receptor subtypes expressed on GABAergic interneurons and Glutamatergic principal neurons within the amygdala and PFC seem to mediate the effects of 5-HT.

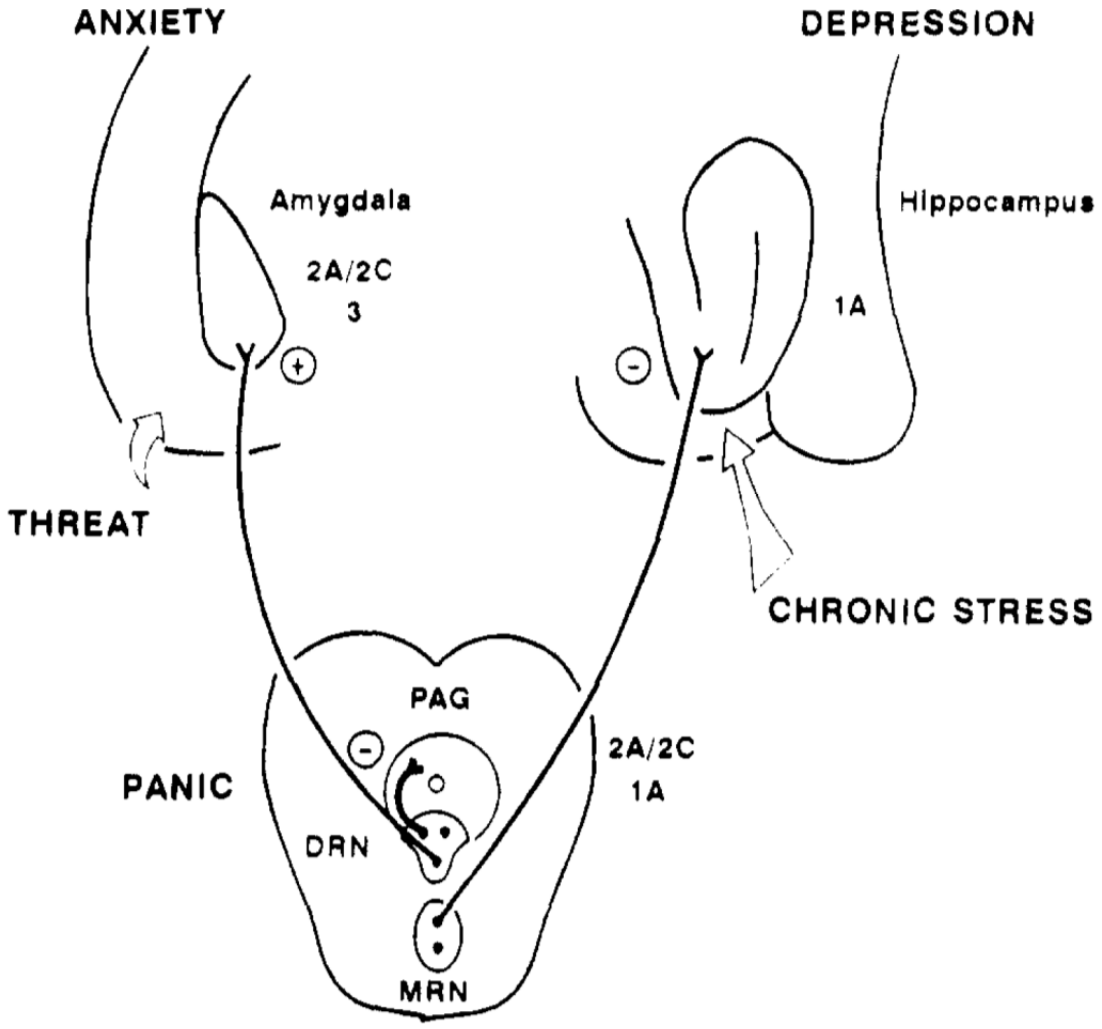

Graeff and Deakin 1996

Fig.1-4 The dual role of 5-HT in anxiety and depression

Localization of 5-HT1A, 5-HT1B, 5-HT2A, 5-HT2C, and 5-HT3A receptors in the DRN-mPFC-amygdala circuit. These receptor subtypes exhibit a complex and often overlapping pattern of localization within the circuits. DRN = dorsal raphe nucleus, mPFC = medial prefrontal cortex.

1.6 Hypothesis to use 5-HT deficient mouse models

A huge body of studies has linked alterations in the 5-HT system with psychiatric disorders. The risk to develop depression following environmental stress is increased by genetic susceptibility factors involving a set of serotonergic system related genes for review see (Waider et al., 2011). However, the molecular mechanisms underlying the pathophysiology of depression are merely understood. Mouse models of an altered 5-HT system exhibit alterations in anxiety- and depression-like behaviors. In order to investigate the role of a complete 5-HT deficiency we generated and analyzed mice deficient in the neuronal (5-HT) synthesis from early prenatal developmental stages by deletion of the fifth Exon of the *Tph2*. In the first part of this thesis the knockout of *Tph2* was confirmed by histological and neurochemical methods and its impact on the GABAergic system was investigated. Furthermore, I establish an approach to investigate molecular determinants of formerly 5-HT neurons based on the expression of fluorescent marker proteins in 5-HT neurons.

In the second part of this thesis, I intend to show the first basic behavioral consequences of the *Tph2* knockout in mice, and aim to discuss my histological findings together with the behavioral data, which were kindly provided by Dr. Lise Gutknecht and Mrs. Sandy Popp.

2. Materials and Methods

2.1 Material

2. 1.1 Mice

Mice were housed according to the European Community guidelines for animal care (DL 116/92, application of the European Communities Council Directive 86/609/EEC). Generation and genotyping of *Tph2*$^{-/-}$ mice has been described in Gutknecht et al. (2008) with a genetic background of 97% C57Bl/6N and 3% Sv129Ola. Male *Tph2*$^{-/-}$, *Tph2*$^{+/-}$ and *wt* mice on a mixed Sv129/Bl6 N (3/97 %) background three months of age were used.

Table 2 Genetically modified mouse strains used within this thesis

Mouse line	Comment	References
B6.*Tph2*$^{-/-}$	*Tph2* deficient mice	(Gutknecht et al., 2008)
B6.*Pet-1*cre	Expression of Cre recombinase in 5-HT neurons by the *Pet-1* promoter	(Dai et al., 2008)
B.6.CAG.EGFP	Transgenic mice carrying an inducible eGFP cassette	(Nakamura et al., 2006)

Cross-fostering of three different mouse lines (see Table 2) was carried out to generate 5-HT system specific eGFP expressing *Tph2*$^{-/-}$ mice. This results in expression of the Cre recombinase driven by the 5-HT specific promoter of the *Pet-1* transcription factor. This will remove the stop cassette in the B.6.CAG.eGFP transgene and lead to strong *Pet-1* promoter specific expression of eGFP by the CMG promoter.

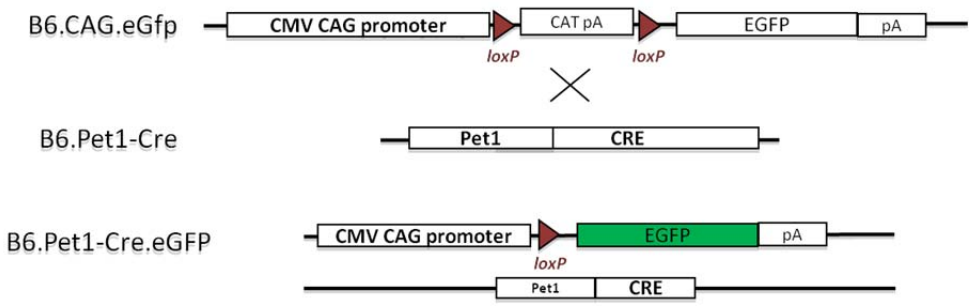

Fig. 2-1 Crossing scheme to generate mice with 5-HT system specific expression of EGFP

2.1.2 Tissue

For in situ hybridization (ISH), brains were immediately frozen in dry ice-cooled isopentane. For immunohistochemistry brains were perfused transcardially with 4% PFA in PB (ph = 7.3) and post fixed within the same fixative over night. Brains were cryopreserved in 20% sucrose solution and stored at -80°C. For ISH and IHC, native or fixated tissues were cut into 16-20 µm sections at -20 °C using a cryostat (HM 500 O, Microm). Slices were mounted onto superfrost plus slides (Menzel, Braunschweig, Germany) and stored at -80 °C for later use.

2.1.3 Oligodesoxynucleotids

Oligodesoxynucleotids for genotyping (Tab) were obtained from MWG-Biotech (Ebersberg, Germany)

Table 3 Primer used for mouse genotyping

Name	Sequence 5'-3'	product size	Use
JAXegfp3	tccttgaagaagatggtgcg	173bp	Screening for the eGFP transgene
JAXegfp5	aagttcatctgcaccaccg		
CRE-L-F	gcgcggtctggcagtaaaaac	117bp	Screening for the Cre

CRE-L-R	cgccgcataaccagtgaaaca		recombinase transgene
IL2-F	ctaggccacagaattgaaagatct	324bp	Internal positive control in the Cre PCR
IL2-R	gtaggtggaaattctagcatcatcc		
3'Del	tggggcatctcaggacgtagtagt	*Wt* = 437bp -/- = 387bp	Detection of *Tph2 wt* and -/- Alleles
3'Over	caccccaccttgcagaaatgttta		
5'Rev	tggggcctgccgatagtaacac		

2.2 Methods

2.2.1 High pressure liquid chromatography (HPLC)

Four month old *Tph2*$^{-/-}$, *Tph2*$^{+/-}$ and *wt* mice were perfused for 10 min with PBS and brains were immediately frozen onto dry ice. Dissected frozen brain regions were solubilized by sonification in transmitter buffer (150 mM H_3PO_4, 500 µM DTPA) and centrifuged (36000g, 20 min, 4°C). Monoamine neurotransmitters and their metabolites were measured by an Agilent 1100 HPLC system. This consisting of EC 250/4.6 Nucleosil 100-3-C18 reversed-phase columns (Machery-Nagel, Düren, Germany) and an electrochemical detector (Machery-Nagel, Düren, Germany), which was adjusted to 0.75 V. Composition of mobile phase was 90% 0.65 mM octanesulfonic acid, pH 3.5, 10% methanol, 0.5 mM triethylamine, 0.1 mM EDTA and 0.1M NaH_2PO_4. For GABA and glutamate measurements, a modified precolumn derivatisation using ortho-phthaldialdehyde (OPA) (Alltech-Grom GmbH, Rottenburg-Hailfingen, Germany) was utilized. Briefly, 10 µl of supernatant were mixed with OPA reagent for derivatisation and injected in an Agilent 1100 HPLC system equipped with a Nucleosil 150/4.6 NUCLEODUR C-18 Gravity, 3 µm column (Machery-Nagel, Düren, Germany) as stationary phase. Mobile phase A consisted of 25 mM phosphate buffer (pH 6.8) with 0.5% of tetrahydrofurane (THF) and mobile phase B of 40 mM phosphate buffer (pH

6.8), 27% methanol and 18% acetonitril. Performed gradient was: 0-3 min 100% A, during 3-30 min up to 100% B, 30-35 min 100% B. Fluorescence detection was used for quantification with an excitation wavelength of 330 nm and detected emission at 450 nm in combination with L-norvalin as internal standard. For quantitative data assessment, HP ChemStation for LC (Machery-Nagel, Düren, Germany) was used.

2.2.3 In situ Hybridization

Brains were frozen directly in dry ice-cooled isopentane and stored at -80 until use. GAD 65/67 cDNA fragments generated by PCR from 3´UTR and cloned in pGEMT vector (Promega, Madison, USA) were used to generate sense and antisense specific digoxygenin (DIG) labeled cRNA probes using DIG RNA labeling kit (Roche, Mannheim, Germany). After fixation for 5 min in freshly prepared cold 4% paraformaldehyde (PFA) in 0.1 M PBS 18 µm sections were rehydrated and treated with 0.02 N HCl. After washing with 2X SSC, the sections were incubated with freshly prepared 0.25% acetic anhydride in 0.1 M triethanolamine for 20 min and blocked with prehybridization solution (50% deionized formamide, 4X SSC, 1X Denhardt's solution, 10% dextransulfat and 250 µg/ml denatured salmon sperm DNA) before DIG-labeled antisense cRNA (10-20 ng/µl) for 16-18 h at 60°C was added. After RNAse A treatment (40 µg/ml) in 1 mM EDTA at 37°C for 30 min, sheep anti-DIG alkaline phosphatase (aP) conjugated antibody for 1h followed by signal detection with 4-nitro blue tetrazoliumchloride (NBT)/ 5-bromo-4-chloro-3-indolyl phosphate (BCIP) solution (Roche, Mannheim, Germany).

2.2.4 Immunohistochemistry

Brains were fixed with 4% PFA in PBS, pH 7.5 by transcardial perfusion, post-fixed over night, cryo-preserved in 20% sucrose and frozen in dry ice cooled isopentane. Brains were sectioned with a cryotome and mounted onto microscope slides covered with 0.3% gelatin solution with 0.05 % chromium potassium sulfate. Coronal serial sections of 18 µm thickness from the hippocampus of 6 mice per genotype and the amygdala of 5 mice per genotype spaced 144 µm were cut and kept frozen at -80°C until use. Antigen retrieval was performed at 95°C for 10 min in 10 mM citrate buffer (pH 6.0) containing 0.05% Tween-20. Unspecific binding sites were saturated with a blocking solution (BS) containing 5% NGS, 2% FBS and 0.25% Triton-X in TBS, for 1 hour. Slides were double stained using rabbit anti-GAD 65/67 (Millipore, Billerica, USA) and mouse anti-PV (Swant, Marly, Switzerland) as primary antibodies. They were diluted together in BS at 4°C overnight. For simultaneous primary antibody detection the TANDEM™ IHC, staining and detection kit (Epitomics, Burlingame, USA) was used. Specific mouse and rabbit polymers coupled to peroxidase and alkaline phosphatase were applied onto the slides for 30 min. GAD 65/67 positive neurons were visualized with diaminobenzidine (DAB) (brown staining) and PV neurons by Fast Red (red staining). Afterwards Nissl counterstaining in 0,1% cresyl violet for 15 min was applied on double stained sections and differentiated in an increasing ethyl alcohol series (70%, 95%, 100%) for 15 sec each before clearing in 1:1 xylene/isopropanol for 5min. Slides were mounted permanently with Vitro-Clud (Langenbrinck, Emmendingen, Germany). Brain structures were delineated with contours in Nissl counterstained sections according to the mouse brain atlas (Franklin and Paxinos, 1997). The amygdala is a complex structure consisting of multiple subnuclei. Here we performed cell counting from the portion of the BLC that is surrounded by the amygdalar capsule (amc). This includes the lateral nucleus and the basolateral nucleus from Bregma -0.58 until Bregma -2.12 without the basomedial nucleus (BMA). In addition, the BLC extends until Bregma -2.96 this part was not clearly

distinguishable and excluded from our analysis. The dorsal Hippocampus was analyzed from its first appearance around Bregma –0.58 in the following three serial sections, which allowed to delineate the different hippocampal layers and regions.

Since PV immunoreactivity obscured GAD staining in double labeled neurons, which have been documented to represent a subgroup of GABAergic neurons in mice (Davila et al., 2008) The number of brown (GAD 65/67 positive) on the one hand and red (PV positive) cells on the other hand were counted separately on double stained sections. The number of GABAergic neurons was calculated as the sum of GAD 65/67 positive and PV neuron numbers.

2.2.5 Immunofluorescence labeling

Brains were fixed with 4% PFA in PBS, pH 7.5 by transcardial perfusion, post-fixed over night, cryo-preserved in 20% sucrose and frozen in dry ice cooled isopentane.

Immunofluorescence detection was performed on frozen 20-30 μm thick coronal serial sections mounted onto microscope slides covered with gelatin and kept frozen at -80 until use. Antigen retrieval was performed at 95°C for 10 min in 10 mM citrate buffer (pH 6.0) containing 0.05 % Tween-20. Sections were blocked with BL for 1h and afterwards incubated with primary antibodies listed in Table 4 in BL at 4°C over night. After three 5 min washes, TBS secondary antibodies (listed in Table 4) were applied in BL, diluted ½ in TBS, for 1h 30 min. After three 5 min washes cell nuclei were counterstained by DAPI (300 nM in TBS) and mounted in Fluoro-Gel (BioMeda, Forster City, USA).

Immunohistofluorescent colocalisation of Tph1 or *Tph2* specific antibodies to validate the specificity of the in-house made rabbit anti Tph1 and *Tph2* specific antibodies with Tph1/2 was carried out separately on adjacent mouse raphe sections with a well validated non isoform discriminative Tph specific antibody sheep anti Tph1/2.

Table 4 Antibodies used in immunohistochemistry and immunofluorescence

	Antibodies	**Concentration (IHC)**	**Concentration (IF)**	**Origin**
Primary Antibodies	ms anti Parvalbumin	1:1000	-	Swant
	rabbit anti *Tph2*	1:1000	1: 1000	in-house
	sheep anti *Tph2*/Tph1	-	1:300	Chemicon
	rabbit anti Tph1	1:1000	1:300	in-house
	rb anti GAD65/67	1:500	-	Chemicon
	rabbit anti 5-HTT	1:750	1:500	Calbiochem
	rabbit anti 5-HT	1:5000	1:5000	Immunostar
	chicken anti GFP	-	1:500	Abcam
	mouse anti Dig		1:500	Roche
Secondary Antibodies	goat anti rabbit	-	1:400	Invitrogen
	goat anti chicken	-	1:400	Invitrogen
	goat anti sheep	-	1:400	Invitrogen
	goat anti rabbit	-	1:400	Invitrogen
	goat anti mouse	1:2	-	Epitomics
	goat anti rabbit	1:2	-	Epitomics

2.2.6 Microscopy

For bright field photomicrographs a motorized Olympus BX 51 equipped with a charge-coupled device (CCD) camera system was used with the Neurolucida software (MicroBrightfield, Magdeburg, Germany). For double fluorescence images without the use of eGFP, a motorized Olympus BX-40 was used in combination with the CellP^{TM} software (Olympus, Hamburg, Germany). For double fluorescence images including eGFP, staining a Leica SP5 confocal microscope was used.

2.2.7 The stereo investigator

The total number of cells was determined in 6-8 coronal 18 µm thick serial sections spaced 144 µm of the BLC. Total number of cells were counted in Nissl counterstained sections using the optical fractionator method of Stereo investigator (MicroBrightfield, Magdeburg, Germany) in order to avoid counting bias (West, 2001). Total cell numbers were extrapolated by multiplying the number of counts with the serial sampling fraction (ssf), the thickness sampling fraction (tsf) and the area sampling fraction (asf). The total volume of the analyzed regions was calculated by the product of intersectional space and the sum of delineated areas (Gundersen et al., 1988). In order to ensure that the intra- individual variance does not contribute significantly to the inter-individual variance (Keuker et al., 2001), a reasonable sampling scheme resulting in a coefficient of error (CE) < 0.1 for all animals was applied. Therefore, a grid overlaying the BLC of 100x150 µm and optical dissectors of a 30x40x12 µm volume were employed to estimate the total number of cells excluding cells lying within a buffer zone of the first and last three µm of the section. A 40x and 100x oil objective was used on an Olympus BX51 microscope equipped with a charge-coupled device (CCD) camera system.

The total cell densities were calculated for all animals as previously described (Gundersen et al., 1988) by the quotient of estimated number of cells and the total volume of the structure.

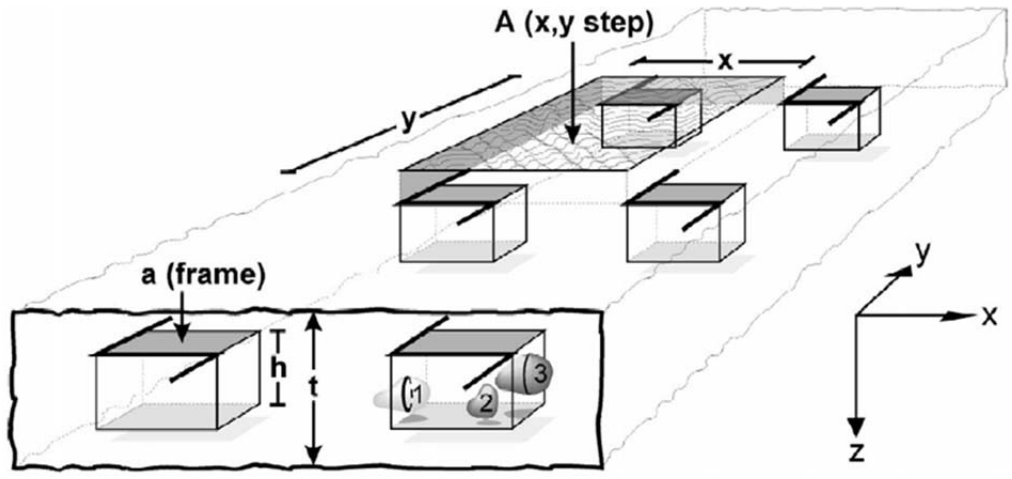

$$N = \sum Q^{-} \cdot \frac{1}{\text{ssf}} \cdot \frac{1}{\text{asf}} \cdot \frac{1}{\text{tsf}}$$

(adapted from Keuker et al., 2001)

Fig.2-2 Estimation of total cell number by the optical fractionator

Cells were counted in optical dissectors, which are spaced within a grid overlaying the region of interest in randomly serial sections. The total number of neurons was calculated by the sum of neurons counted multiplied with the serial section fraction (ssf), the area sampling fraction (asf) and the thickness sampling fraction (tsf). The ssf is the quotient of counted series and the total number of randomly sectioned series. The asf is the quotient of the area of the optical dissector counting frame, a (frame), and the A(x, y step). The thickness sampling fraction is determined by the ratio of the height of the dissector counting frame (h) and the measured section thickness (t). h, height of the optical dissector; t, section thickness; a(frame), area of the optical dissector counting frame; thick black lines, exclusion lines; dark gray frame of optical dissector, top exclusion side.

2.2.8 Fluorescent activated cell sorting (FACS)

The embryonic hindbrain of E17 embryos from the *Tph2 Pet-1*-Cre eGFP line was isolated carefully by an incision within the midbrain-hindbrain boundary in ice cold PBS with 2% glucose. After removal of the meninges to prevent contamination of the stem cell culture by fast growing fibroblasts, the hindbrain was incubated by a small incision in the midbrain hindbrain boundary. The hindbrain was placed into NeuroCultTM Proliferation Medium (STEMCELL Technologies, Grenoble, France) and triturated with a 1 ml plastic tip.

After the supernatant was removed, the tissue was incubated in 300µl ACCUTASE^{TM} (Millipore, Billerica, USA) at 37°C for 10 min and triturated with a 200µl pipette tip (150x) to a single cell suspension. The suspension was centrifuged at 150g for 5 min and the cells were resuspended in 1ml fresh NeuroCultTM Proliferation Medium. The single cell suspension was incubated at 37°C in the dark and afterwards transported 30min to the FACS cell sorter.

Cells were filtered through a 40 µm filter and sorted on a FACS Aria III (Becton Dickinson, Franklin Lakes, USA) equipped with argon laser with an excitation of 200 mW at 488nm. Green fluorescence was detected by a FITC-A Filter set, with a sort pressure of 22 psi with a 70µm nozzle. Aggregates were eliminated by forward scatter height versus width scatter.

2.2.9 Behavioral testing of Tph2$^{-/-}$ mice

All behavioral tests were performed in the Core Unit for Mouse Behavior at the Centre of Experimental Molecular Medicine (ZEMM), University of Würzburg, during the dark period from 12:00 to 21:00 under dim red light illumination. Testing was carried out at 8-10 weeks of age and behavioral tests were separated by one-week intervals to reduce inter-test interactions. All animal protocols have been reviewed and approved by the review board of the Government of Lower Franconia and the University of Würzburg and will be conducted

according to the Directive of the European Communities Council of 24 November 1986 (86/609/EEC).

Unpredictable chronic-mild stress

Eight mice per genotype (Tph2$^{-/-}$, *Tph2*$^{+/-}$ and *wt* controls) were exposed to unpredictable mild stressors according to a fixed weekly schedule (Table 5) for 21 days including overnight illumination, food or water deprivation, a tilted cage (30°) for 3h, an empty bottle for 3h, and three times restraint stress (restricted space within the home cage of 8x8x11cm) for 1h.

Table 5 Time schedule of the chronic mild stress (CMS) procedure

Time	Monday	Tuesday	Wednesday	Thursday	Friday	Saturday	Sunday
09:00			Restraint	Tilted cage	Empty bottle	Tilted cage	Restraint
10:00				Tilted cage	Empty bottle	Tilted cage	
11:00							
12:00				Tilted cage	Empty bottle	Tilted cage	
13:00							
14:00							
15:00		Tilted cage	Empty bottle				Empty bottle
16:00		Tilted cage	Empty bottle				Empty bottle
17:00					Restraint		
Over-night	No Water	Tilted cage	Empty bottle	No Food		Lights On	No Water

Open Field

Mice were placed into the test room 45 minutes before test start into the Open Field consisting of a quadratic PERSPEX XT box (50 cm x 50 cm x 40 cm, semi-permeable to infrared light) as previously described (Post et al., 2011a). The apparatus was illuminated by infrared LEDs from below. Activity monitoring was carried out using an infrared sensitive CCD camera and the computer-based video-tracking software VideoMot 2 (TSE Systems, Bad Homburg, Germany). Therefore, the arena of the Open Field was divided into a 36 cm x 36 cm central zone and the surrounding periphery. Entries into the central zone or periphery were counted when the mouse placed all four paws into the respective zone. Behavior was monitored for an interval of 5 min.

Elevated-Plus Maze

Mice were placed into the room for 10 minutes before testing. Afterwards they were placed into the central platform (5x5 cm) of a gray plastic plus-shaped maze made of PERSPEX XT (semi-permeable to infrared light, TSE Systems, Bad Homburg, Germany) facing toward an open arm (open arm: 30x5 cm, surrounded by a 0.25 cm-high border, closed arms: 30x5 cm, surrounded by 15 cm-high opaque walls) (Post et al., 2011b). The entire apparatus was elevated 60 cm above the floor and illuminated by infrared LEDs from below. Locomotion data was collected for 5 minutes by a video tracking system (VideoMot2, TSE Systems, and Bad Homburg, Germany).

Porsolt Swim Test

The Porsolt swim test was carried out according to a modified method of Porsolt (Porsolt et al., 1977, Cichon et al., 2008). Mice were placed into a water filled glass cylinder (23 cm height, 13 cm diameter). Mice were tested for 5 min monitored by an experienced observer. The time spent on climbing, swimming, and immobility was recorded to determine active vs.

passive stress-coping performance. Mice were considered immobile when floating passively in the water. In addition, duration of immobility was automatically assessed using the ‘‘mobility’’ feature of the Noldus software, EthoVison 1.96 (Noldus Information Technology, Wagingen, NL).

Sucrose preference test

Baseline sucrose consumption/preference was measured for five consecutive days immediately prior to the onset of CMS (basal level). During the test, mice got a free choice between two bottles, one with 2.5% sucrose solution and another with tap water. The consumption of water, sucrose solution, and total intake of liquids was estimated simultaneously in the control (non-stressed) and stressed groups by weighing the bottles every 24h. Sucrose consumption was calculated as the mean sucrose intake per day through a period of five days and expressed as mg sucrose intake per g body weight per day (mg/g/day). The sucrose preference was calculated as percentage of consumed sucrose solution of the total liquid drunk by the following formula: Sucrose Preference = V (Sucrose solution)/V (Sucrose solution) + V (Water) x 100%). Behavioral testing was followed by another sucrose consumption/preference test.

2.2.10 Statistics

For HPLC data statistical significance was tested using one-way ANOVA (indicated by F (df1, df2) values) followed by Tuckey’s post-hoc test. Kruskal-Wallis test followed by Dunn‘s post-hoc for multiple testing was used for interneuron counting and stereological estimation of total cell numbers in BLC. Student’s t-test was used for hippocampal cell counting. The behavioral data were analyzed using ANOVA followed by Tuckey's post hoc

tests for multiple group comparison or paired two-tailed student t-test in case of repeated measures. A p-value $\leqslant 0.05$ was considered as statistical significant. A p-value $\leqslant 0.1$ and $\geqslant 0.5$ was considered as a statistical trend. Outliers were removed after Grubb's test. All data were analyzed using GraphPad Prism version 5.00 (GraphPad Software, San Diego California, USA)

3. Results

3.1 Histochemistry of Tph2$^{-/-}$ mice

Tph2 deficient mice (*Tph2*$^{-/-}$) are viable and do not show apparent increase in premature lethality across their lifespan. Immunohistochemistry with *Tph2*-specific antibodies against the ablated c-terminal part confirmed the deletion of *Tph2* Exon V.

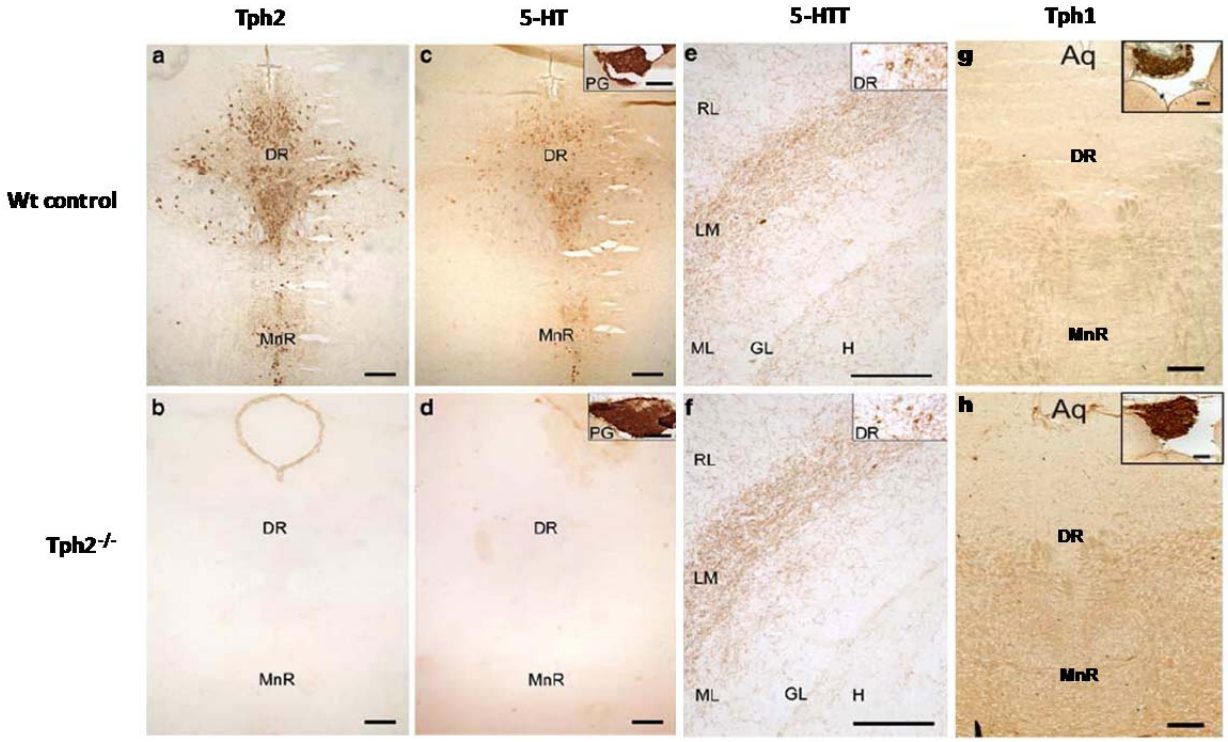

Fig.3-1 Detection of serotonergic markers in *Tph2*$^{-/-}$ mice

Detection of serotonergic-specific markers was performed on coronal brain sections of adult *wt* control (upper row) and *Tph2*$^{-/-}$ mice (lower row). (a) Labeling of *Tph2* demonstrated its complete absence in the raphe of *Tph2*$^{-/-}$ mice. (b) The 5-HT transporter (5-HTT) could be detected in wt and *Tph2*$^{-/-}$ mice, in the raphe as well as along fibers in projection areas, e.g. in the frontal cortex (FC) as shown in (c). (e) Detection of 5-HT in the raphe showed the absence of specific 5-HT immunoreactivity in *Tph2*$^{-/-}$ mice (f). DR: dorsal raphe; MnR: median raphe; RL: stratum radiatum; LM: stratum lacunosum moleculare; ML: molecular layer; GL: granule cell layer; H: hilus; Aq: aqueduct. Bars represent 200 μm.

Complete absence of *Tph2* immunostaining was detected in *Tph2*$^{-/-}$ mice as compared to wildtype (*wt*) littermates (Fig. 3-1 a, b). Loss of *Tph2* resulted in a complete 5-HT deficiency in raphe serotonergic neurons (Fig. 3-1c, d). In contrast, a strong 5-HT-specific signal was observed in the pineal gland of wt and *Tph2*$^{-/-}$ mice (Fig. 3-1 inserts in c, d).

Development of formerly serotonergic neurons was not affected by 5-HT deficiency itself, because immunohistochemistry against the 5-HTT revealed expression of 5-HTT on soma, dendrites and terminals of neurons in a similar pattern in *wt* and *Tph2*$^{-/-}$ mice within the DR and target regions like the dorsal hippocampus (Fig. 3-1 e, f).

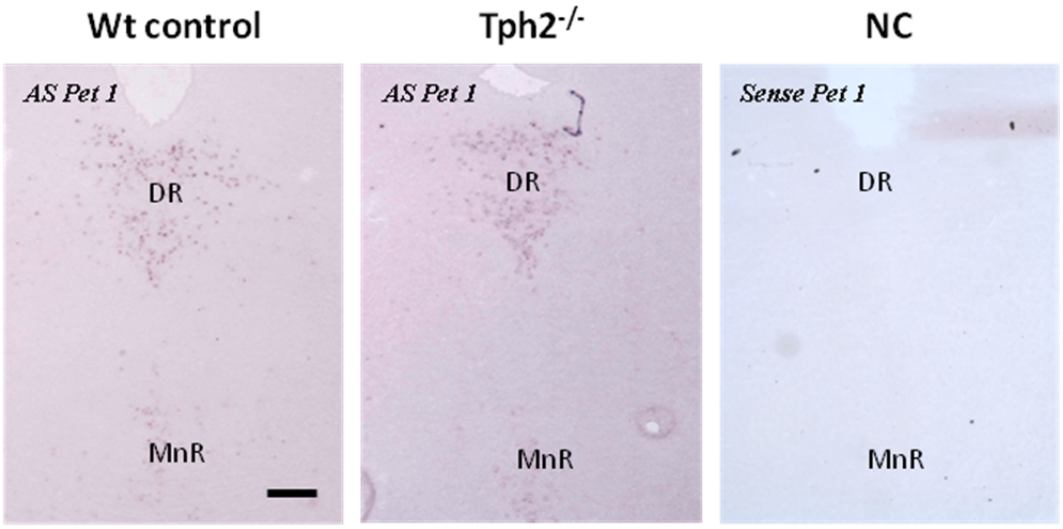

Fig.3-2 Expression of *Pet-1* transcription factor in *Tph2*$^{-/-}$ mice

I*n-situ* hybridization using an anti-sense (AS) probe against the serotonergic-specific transcription factor *Pet-1* demonstrates expression in the raphe of *wt* and *Tph2*$^{-/-}$ mice. In a negative control (NC), using a sense probe (S) of *Pet-1* revealed no signal in the raphe. DR: dorsal raphe, MnR: median raphe. Bars represent 200 μm.

Using in-situ hybridization against the *Pet-1* transcription factor the presence and normal development of 5-HT deficient neurons in the raphe nuclei of *Tph2*$^{-/-}$ mice was confirmed

(Fig. 3-2). A compensatory effect by Tph1 upregulation could be ruled out since Tph1 expression was neither found in the raphe nuclei of *wt* nor in *Tph2*$^{-/-}$ mice although expression was detected in the pineal gland (Fig. 3-1 g, h) as it was found for 5-HT immunostaining.

3.2 Targeting of Tph2 depleted serotonergic neurons

As shown by *Pet-1 in-situ* hybridization, 5-HT neurons of *Tph2*$^{-/-}$ mice develop normally and reside in the raphe nuclei. However, due to the deletion of *Tph2* established markers to identify 5-HT neurons in *Tph2*$^{-/-}$ mice are missing. In order to reveal the nature of 5-HT neurons in *Tph2*$^{-/-}$ mice a new mouse line was established in order to identify formerly 5-HT neurons for further histological and electrophysiological investigations.

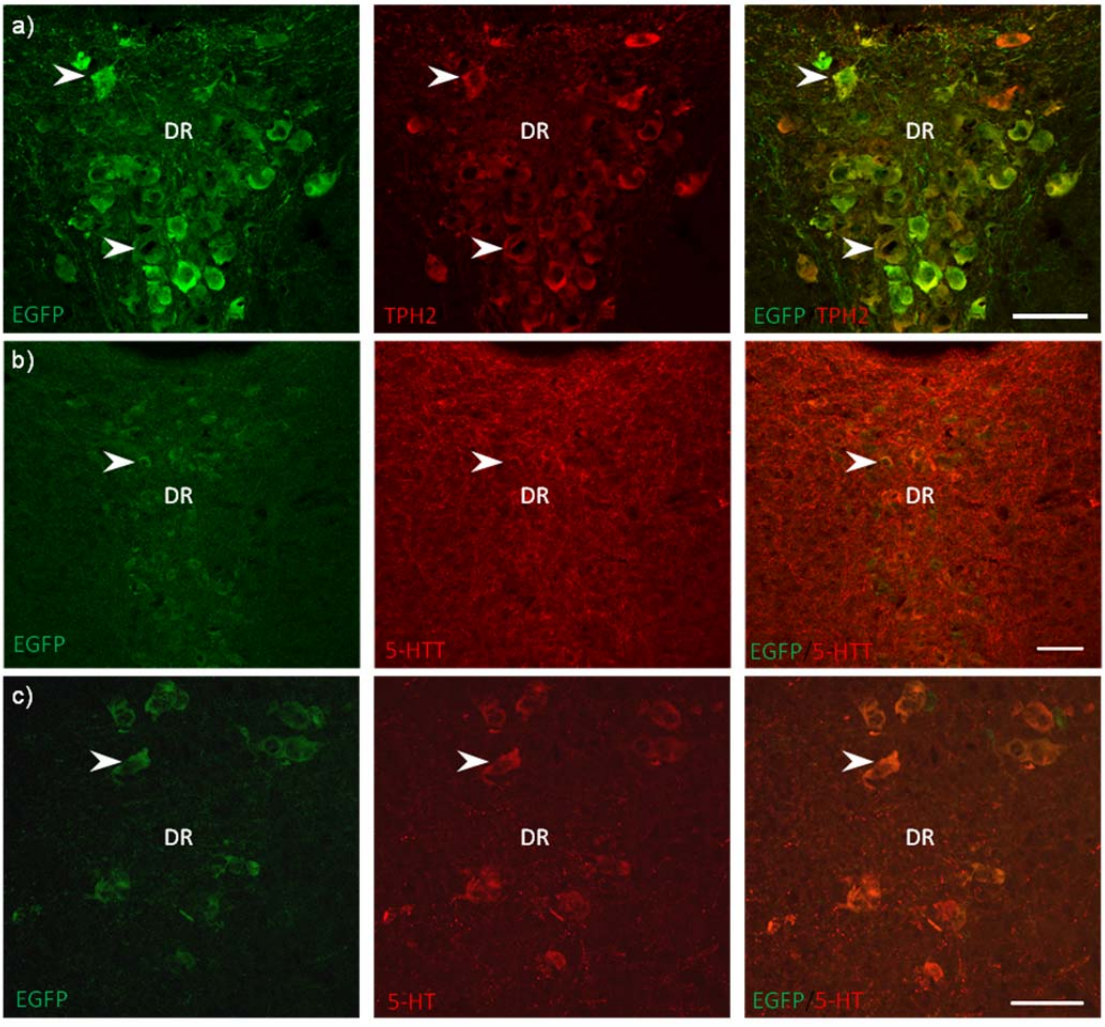

Fig.3-3 Confocal images of *Pet-1*-Cre eGFP transgenic mice
Mice expressing a transgenic construct with an inducible eGFP cassette were crossed with *Pet-1*-Cre transgenic to generate progeny expressing eGFP under the control of the *Pet-1* promoter by Cre recombinase mediated deletion of the CAG stop codon flanked by loxP sites. These mice show double labeling with an anti-Tph2 antibody in nearly all GFP positive neurons (a) of the dorsal raphe nucleus (DR). EGFP and anti 5-HTT double labeling of DR is shown in (b). Higher resolution images of eGFP and 5-HT double labeling are depicted in (c). White arrowheads show double stained cells. Scale bars in (a) and (b) are 100µm in c 50µm.

Therefore, I crossed mice expressing a transgenic construct harboring an inducible enhanced green fluorescence (eGFP) cassette with *Pet-1*-Cre transgenic mice to produce mice expressing eGFP under the control of the *Pet-1* promoter by Cre recombinase mediated deletion of the CAG stop codon flanked by loxP sites (Fig. 2-1).

These mice were characterized by double immunofluorescence labeling against 5-HT system specific markers and eGFP. Virtually all eGFP positive cells showed co-labeling with Tph2 (arrows in Fig. 3-3 b) and 5-HT (arrows in Fig. 3-3 d). Whereas only a few cells showed clear somatic co-labeling with an antibody targeting 5-HTT (arrows in Fig.3-3 d).

These mice were cross-fostered with *Tph2*$^{-/-}$ mice in order to get excess of formerly 5-HT neurons in *Tph2*$^{-/-}$ mice, which is currently under investigation.

In order to reveal if it would be possible to separate 5-HT neurons identified by GFP fluorescence from non-fluorescent cells E17 embryos were sorted by fluorescence activated cell sorting (FACS) and compared to negative control E17 embryos without the eGFP transgene. As a positive control SH-SY5Y cells stably transfected with a vector expressing eGFP under the CMV promoter were used.

Unfortunately, no eGFP positive cells were detected in the FITC-A channel when isolated from E17 embryos. On the other hand, SH-SY5Y neuroblastoma cells, which were stably transfected with an eGFP expressing vector, could be sorted by FITC-A excitation.

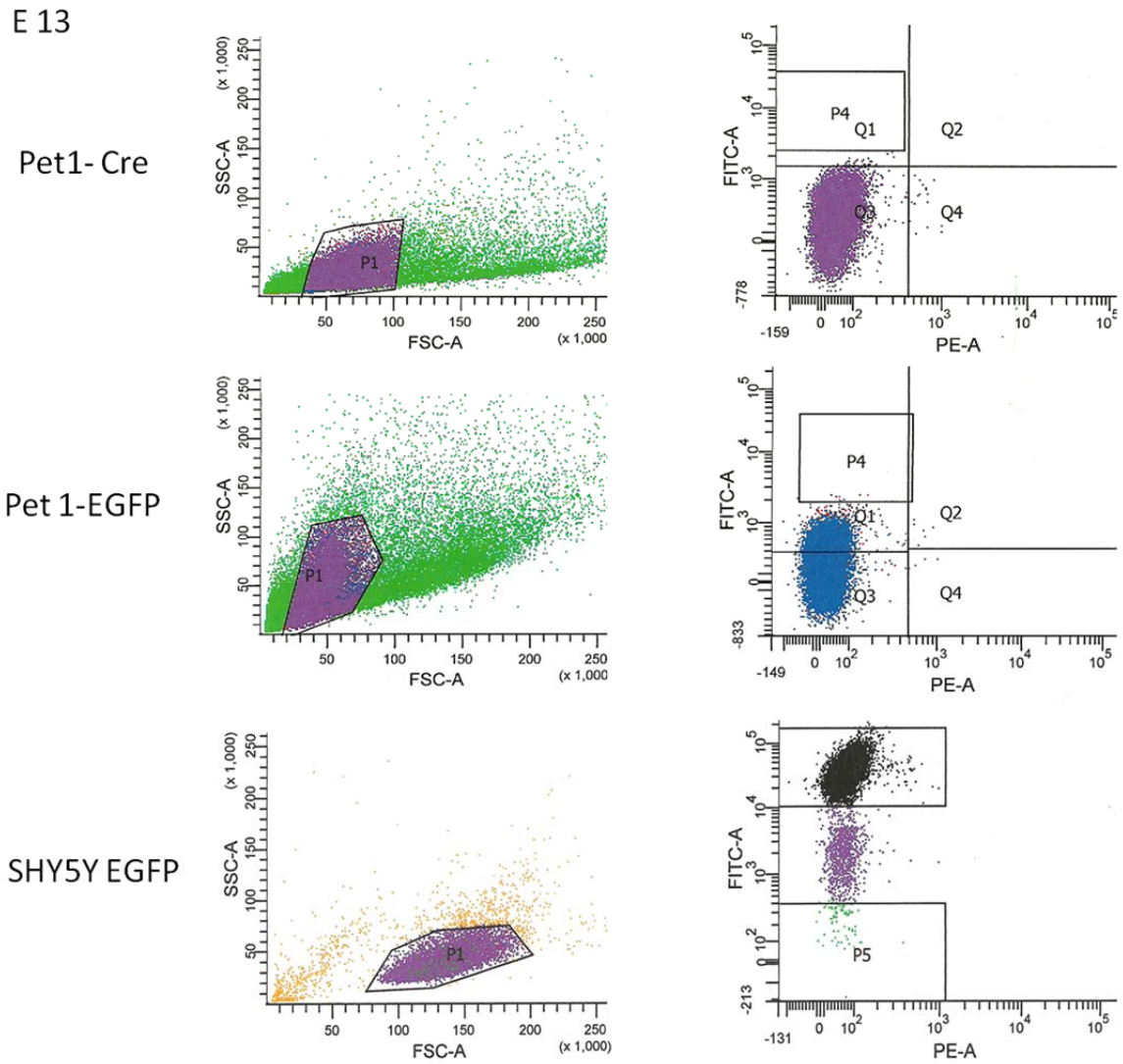

Fig.3-4 Fluorescence activated cell sorting (FACS) of *Pet-1*-Cre.eGFP neurons

Embryos of embryonic day 17 (E17) expressing eGFP under the control of the *Pet-1* promoter were sorted by green fluorescence and compared with a negative control of embryos lacking the eGFP reporter transgene. As a positive control, stably transfected eGFP expressing SH-SY5Y cells were used. Single cells were identified by size in the forward (FSC) and granular structure in the side scatter (SSC). EGFP positive cells were identified within gate 4 (P4) by a standard FITC filter.

3.3 Transmitter measurements in Tph2$^{-/-}$ mice

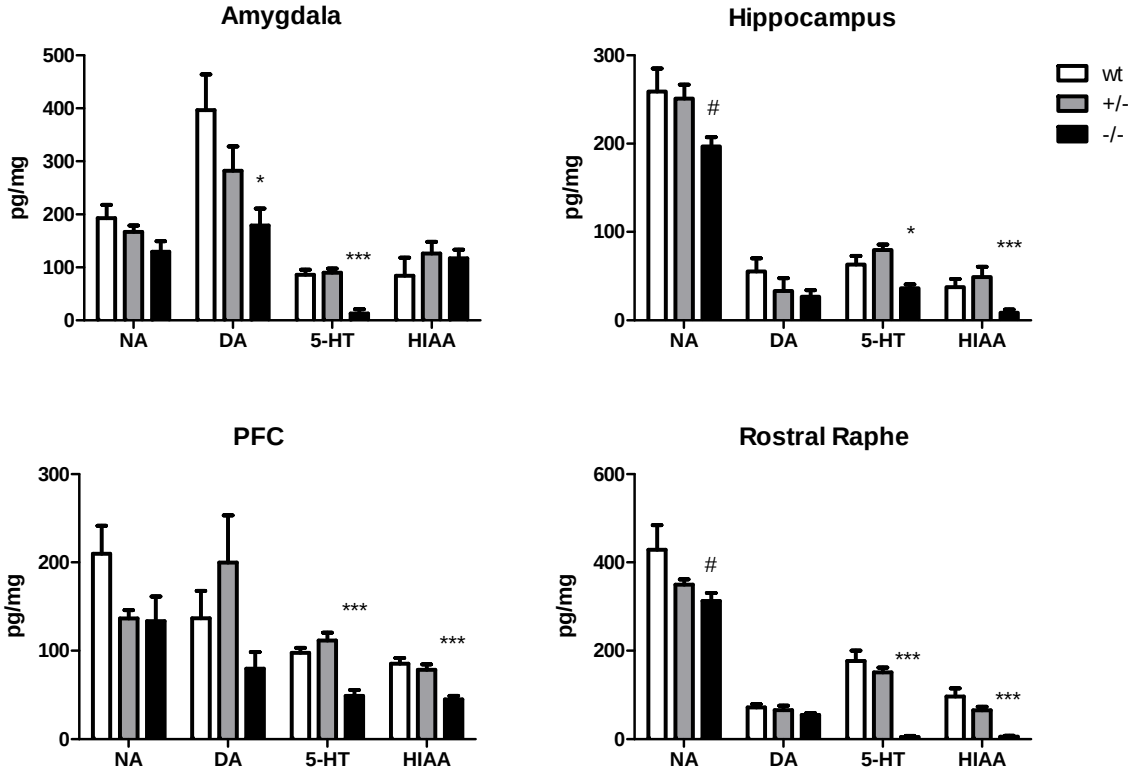

Fig.3-5 Monoaminergic neurotransmitter concentrations in different brain regions
HPLC analysis of norepinephrine (NE), dopamine (DA), 5-HT and its metabolite 5-hydroxyindoleacetic acid (5-HIAA) in four different brain regions (n=8). One-way ANOVA followed by Tuckey's test: $^{\#}$ <0.1; *p<0.05; **p<0.01; ***p<0.001. Data are presented as means ± SEM.

To investigate the effects of *Tph2* inactivation on brain 5-HT concentrations and other monaminergic neurotransmitter systems, high-performance liquid chromatography (HPLC) combined with electrochemical detection of different brain regions was used (Fig. 3-5).

In all brain regions tested *Tph2*$^{-/-}$ mice exhibit a significant reduction in 5-HT levels compared to *wt* controls, especially in the rostral raphe with up to 98% ($F(2,21) = 36,89$; $p \leq 0.0001$) and the amygdala with 84% ($F(2,21) = 25,91$; $p \leq 0.0001$). Although some remaining 5-HT could be detected in hippocampus and PFC in *Tph2*$^{-/-}$ mice ($F(2, 21) = 17, 38$; $p \leq 0.0001$). In

Tph2$^{+/-}$ mice, 5-HT concentrations were not changed significantly. 5-HIAA concentrations were affected similar to 5-HT concentrations except for the amygdala, which displayed unaltered 5-HIAA levels, indicating an altered amygdala specific turnover rate. Additionally, we measured other monoaminergic neurotransmitters closely connected to the 5-HT system, namely noradrenalin (NA) and dopamine (DA). Although reduced in all limbic brain regions of *Tph2*$^{-/-}$ mice, significance was only reached for DA in the amygdala ($F(2, 21) = 4{,}655$; $p = 0.0212$) whereas a trend to reduced NA was reached in *Tph2*$^{-/-}$ mice only in the hippocampus ($F(2, 21) = 3, 32$; $p = 0.0557$) and the rostral raphe ($F(2, 21) = 2, 92$; $p = 0.0763$).

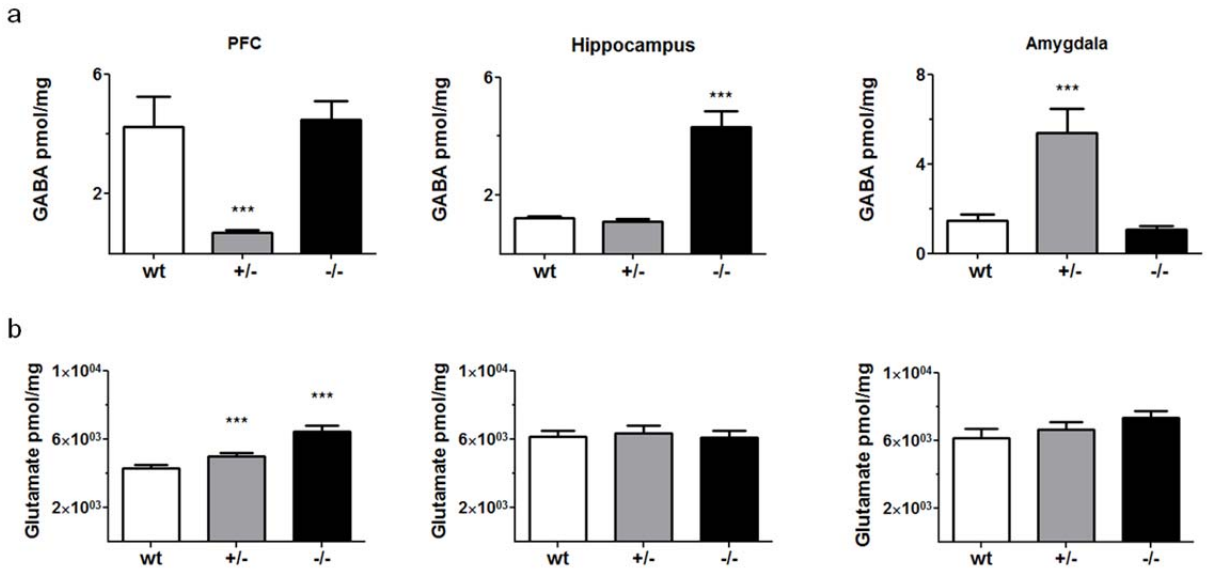

Fig. 3-6 GABA and Glutamate concentrations across brain regions in *Tph2*$^{-/-}$ mice

a) Total concentrations of GABA were measured by high-performance liquid chromatography (HPLC) in different brain regions involved in emotion regulation, including prefrontal cortex (PFC), amygdala and hippocampus in *Tph2*$^{-/-}$ and *Tph2*$^{+/-}$ mice and *wt* controls. b) Concentrations of glutamate were measured in PFC, amygdala and hippocampus. Bars indicate mean ± SEM with N = 8. One-way ANOVA followed by Bonferroni's post-hoc test: ** = $0.01 \geq p > 0.001$, *** = $p < 0.001$

To study the effect of 5-HT depletion on the GABAergic system, HPLC analysis combined with fluorescence detection of GABA in *Tph2*$^{-/-}$, *Tph2*$^{+/-}$ and *wt* control mice in several brain

regions involved in emotion regulation was performed. In parallel, the amino acid glutamate, the main activating neurotransmitter of the brain, was measured. *Tph2*$^{+/-}$ mice showed increased concentrations of GABA in the amygdala ($F(2, 20) = 11.85$; $p = 0.0004$) compared to *Tph2*$^{-/-}$ and *wt* mice (Fig. 3-6a). This effect was reversed in the PFC, with GABA concentration being decreased in *Tph2*$^{+/-}$ compared to *Tph2*$^{-/-}$ mice and *wt* controls. In contrast, the concentration of hippocampal GABA was increased in *Tph2*$^{-/-}$ mice ($F(2, 21) = 31.09$; $p \leq 0.0001$) compared to *Tph2*$^{+/-}$ mice and *wt* controls. However, GABA concentrations within the PFC and amygdala were not changed in *Tph2*$^{-/-}$ mice compared to *wt* controls. Additionally, concentrations of glutamate were determined in PFC, amygdala and hippocampus, which were unaffected by genotype in amygdala ($F(2, 21) = 0.96$; $p = 0.3991$) and hippocampus ($F(2, 21) = 0.12$; $p = 0.8897$) but increased in the PFC ($F(2, 21) = 9.89$; $p = 0.0009$) of *Tph2*$^{-/-}$ mice compared to Tph2$^{+/-}$ and wt controls (Fig. 3-6 b).

3.4 5-HT receptor expression and activation

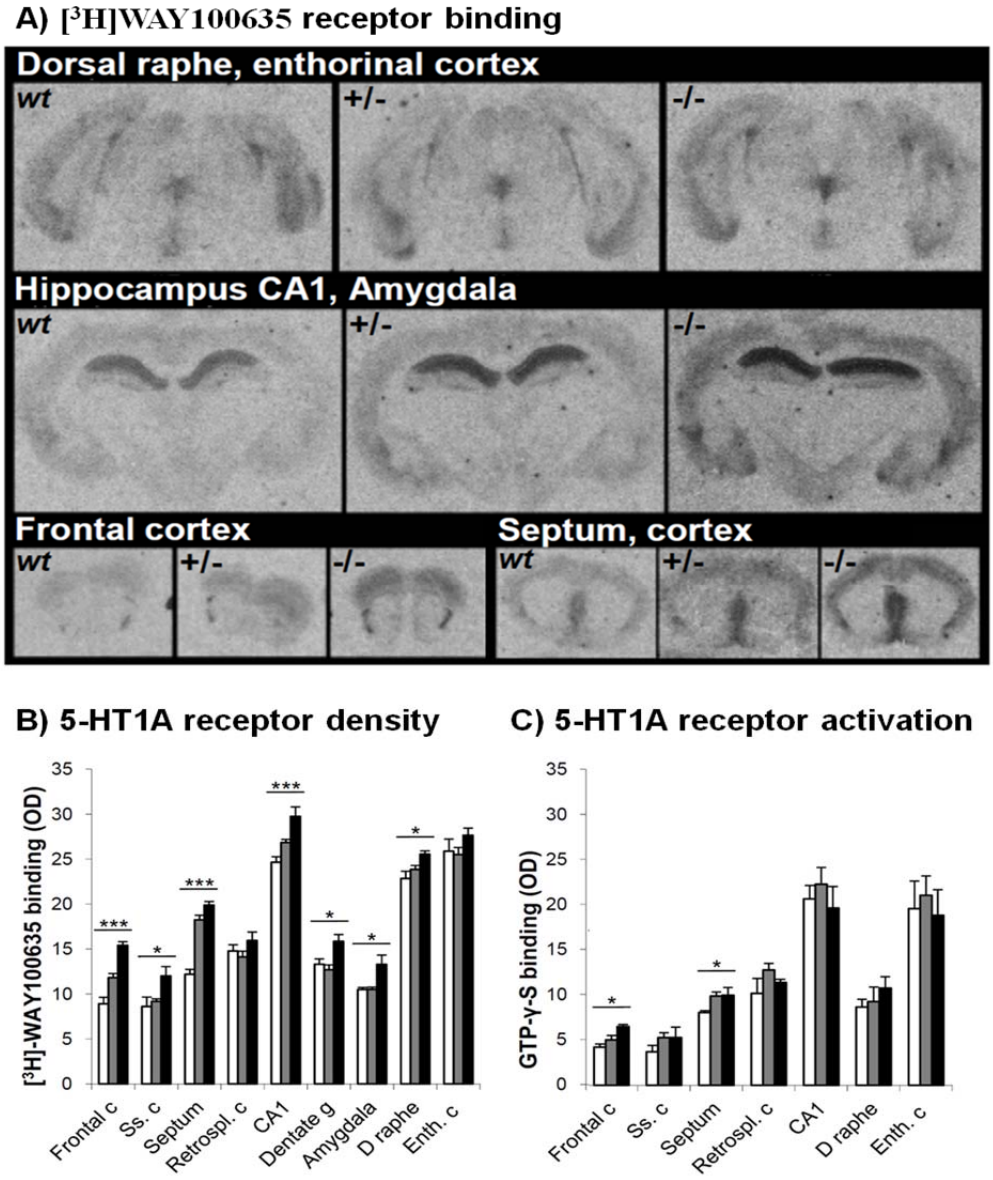

Fig.3-7 Density and activation of 5-HT1A receptors in *Tph2*$^{-/-}$ mice

Representative photomicrographs following the binding of [3H] WAY100635 to 5-HT1A receptors on coronal sections of DR, hippocampus, frontal cortex and septum of *Tph2*$^{-/-}$, *Tph2*$^{+/-}$ and *wt* control mice (a). Optical density of 5-HT1A receptor binding with specific antagonist [3H] WAY100635 in (b) and of 5-HT1A-receptor-mediated increase in [35S] GTP-γ-S binding after stimulation (c).

C: cortex, Ss: somatosensory, Retrospl: retrosplenial, CA1: cornu ammonis area 1 of hippocampus, g: gyrus, D: dorsal, Enth: enthorinal, Caud put: caudate putamen, (d) Data are presented as means ± SEM (n=5). One-way ANOVA followed by Bonferonni post-hoc: *p<0.05, **p<0.01, ***p<0.001. (kindly provided by Lise Gutknecht)

To investigate if 5-HT depletion affects 5-HT_{1A} receptor expression autoradiography with the selective 5-HT1A receptor antagonist [3H]WAY 100635 was performed resulting in increased density of 5-HT1A receptors in *Tph2*$^{-/-}$ mice compared to *Tph2*$^{+/-}$ and *wt* controls in most brain regions tested (Fig. 3-7 a, b). Especially in frontal cortex (+73%;$F(2,12)=34.88$, $p<0.001$), septum (+63%; $F(2,12)=67.1$, $p<0.001$), hippocampus (+19-22%; $F(2,12)=6.7$, $0.04<p<0.001$) and amygdala (+15%; $F(2,12)=8.0$, $p<0.05$) 5-HT1A postsynaptic heteroreceptors were increased compared to *wt* control mice. Furthermore, presynaptic 5-HT1A autoreceptors on 5-HT neurons in the DR were increased (+12%; $F(2, 12)=5.6$, $p=0.016$). In a parallel experiment, 5-carboxamidotryptamine (5-CT) was used as an agonist of 5-HT1A receptors to stimulate [35S] GTP-γ-S coupling (Fig. 3-7 c). This resulted in an increase in [^{35}S]GTP-γ-S in the FC (+54%, $F(2,12)=4.0$, $p=0.04$) of *Tph2*$^{-/-}$ mice as well as in the septum of *Tph2*$^{-/-}$ (+24%, $F(2,12)=4.99$, $p=0.04$) and of *Tph2*$^{+/-}$ mice (+23%, $F(2,12)=34.88$, $p=0.048$) compared to *wt* controls. The [35S] GTP-γ-S labeling was completely prevented by the 5-HT1A antagonist WAY 100635 ensuring specificity of 5-HT1A receptor stimulation by [35S] GTP-γ-S. In brain regions showing small 5-HT1A density effects like DR, hippocampus and amygdala differences in [35S] GTP-γ-S coupling were not significant.

3.5 Interneuron cells numbers

3.5.1 Interneuron numbers in the amygdala

Since the BLC is a structure critically involved in mediating anxiety-like behavior and *Tph2*$^{-/-}$ mice exhibit genotype-dependent differences in GABA concentrations in the amygdala, an estimation of GABAergic neuron numbers in the BLC region was performed. Immunohistochemical detection of GAD65/67 neurons and PV neurons (Fig. 3-8) by co-immunostaining with both antibodies identified GAD 65/67-specific neurons by an intense brown precipitate around the nucleus. These were distinguishable from cells with GAD 65/67-specific fiber contacts on the soma (Fig. 3-8 c-e). PV neurons were detected by an intense, red and cell-shaped cytoplasmatic precipitate around the nucleus throughout the BLC and clustered primarily in the basolateral nucleus of the BLC of all genotypes (Fig. 3-8 c-e).

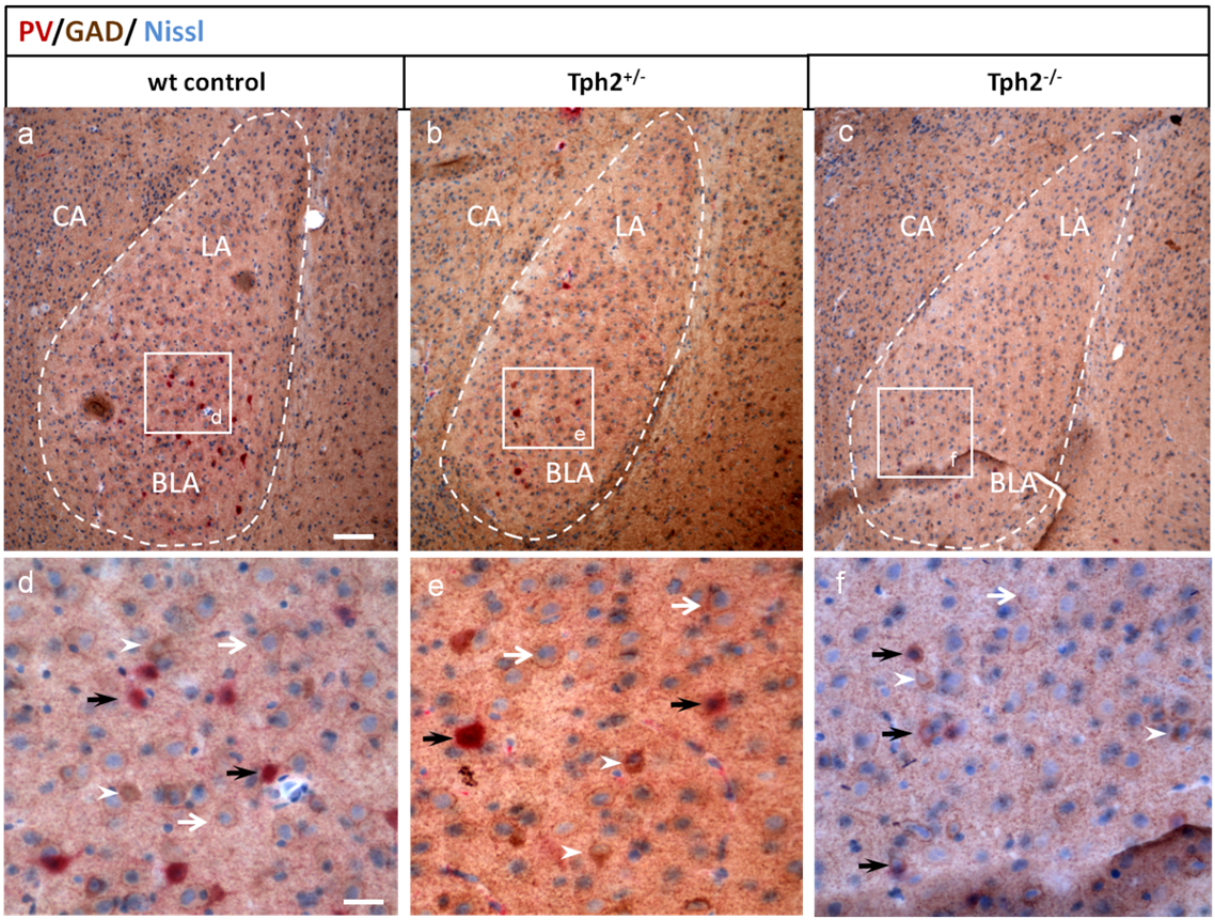

Fig.3-8 Parvalbumin (PV) and glutamic acid decarboxylase (GAD) 65/67 immunostaining. Pictures (a-c) show the basolateral amygdaloid complex (BLC) consisting of the lateral (LA) and the basolateral nucleus (BLA) at –1.58 from bregma in *wt, Tph2*$^{-/-}$ and *Tph2*$^{+/-}$ animals. Higher resolution images in (d-e). White arrowheads indicate single labeled GAD 65/67-specific brown neurons. Black arrows show red PV neurons. Normal white arrows show somatic targets of GAD 65/67-specific fibers onto unstained cells. Lines indicate the boundaries of the (BLC). Scale bar in a = 250 μm and in d= 50μm.

As expected, not all GAD 65/67-specific neurons were PV positive with most PV neurons located within the dorsolateral part of the BLC (Fig. 3-8 a). Co-staining of GAD 65/67 and PV in neurons was not clearly distinguishable from single-labeled PV neurons in controls without one of the primary antibodies. The red precipitate seemed to cover the brown GAD 65/67 cytoplasmatic staining around the nucleus, and made it impossible to distinguish cytoplasmatic GAD/PV co- localization from GAD 65/67-specific fibers in close contact to PV neurons (Fig. 3-8 e-d). Therefore, red-labeled PV neurons and single-labeled brown GAD 65/67-specific cells were counted separately. This revealed a trend towards reduced GAD 65/67-specific cells in the BLC of *Tph2*$^{-/-}$ mice compared to *Tph2*$^{+/-}$ and *wt* mice ($H_{(3)} = 5.42$; $p = 0.067$)(Fig. 3-9 b) whereas PV neurons were not significantly reduced ($H_{(3)} = 1.82$; $p = 0.403$) (Fig. 3-9 a). Based on the assumption that PV neurons represent a subpopulation of GABAergic neurons in mice (Davila et al., 2008), the number of GAD 65/67-specific neurons and of PV neurons were added up to evaluate the total number of GABAergic neurons. Density ($H_{(3)} = 6.02$; $p = 0.049$) and number ($H_{(3)} = 8.43$; $p = 0.037$) of GABAergic neurons were significantly reduced in the BLC of *Tph2*$^{-/-}$ mice compared to *Tph2*$^{+/-}$ and *wt* mice (Fig. 3-9 e and c). No differences in the percentage of PV, which accounted for 25% of total GABAergic neurons in the BLC across genotypes, were detected (Fig. 3-9 f). Specificity of the staining was confirmed by a negative control omitting both primary antibodies (Fig. 3-12). No unspecific cell-like brown staining was visible for both red and brown staining in a negative control omitting both antibodies, although intrinsic alkaline phosphatase activity

caused unspecific red staining around blood capillaries, which was absent in a control omitting the primary anti-PV antibody while applying both secondary antibodies (Fig. 3-12). Finally, the total number of cells was estimated by stereology in the BLC of Nissl counterstained sections. These estimates represent neurons, glia and other cell types. Furthermore, the volume of BLC was estimated. Neither the total number of cells nor the total volumes showed significant differences between genotypes (Fig. 3-9 g, d).

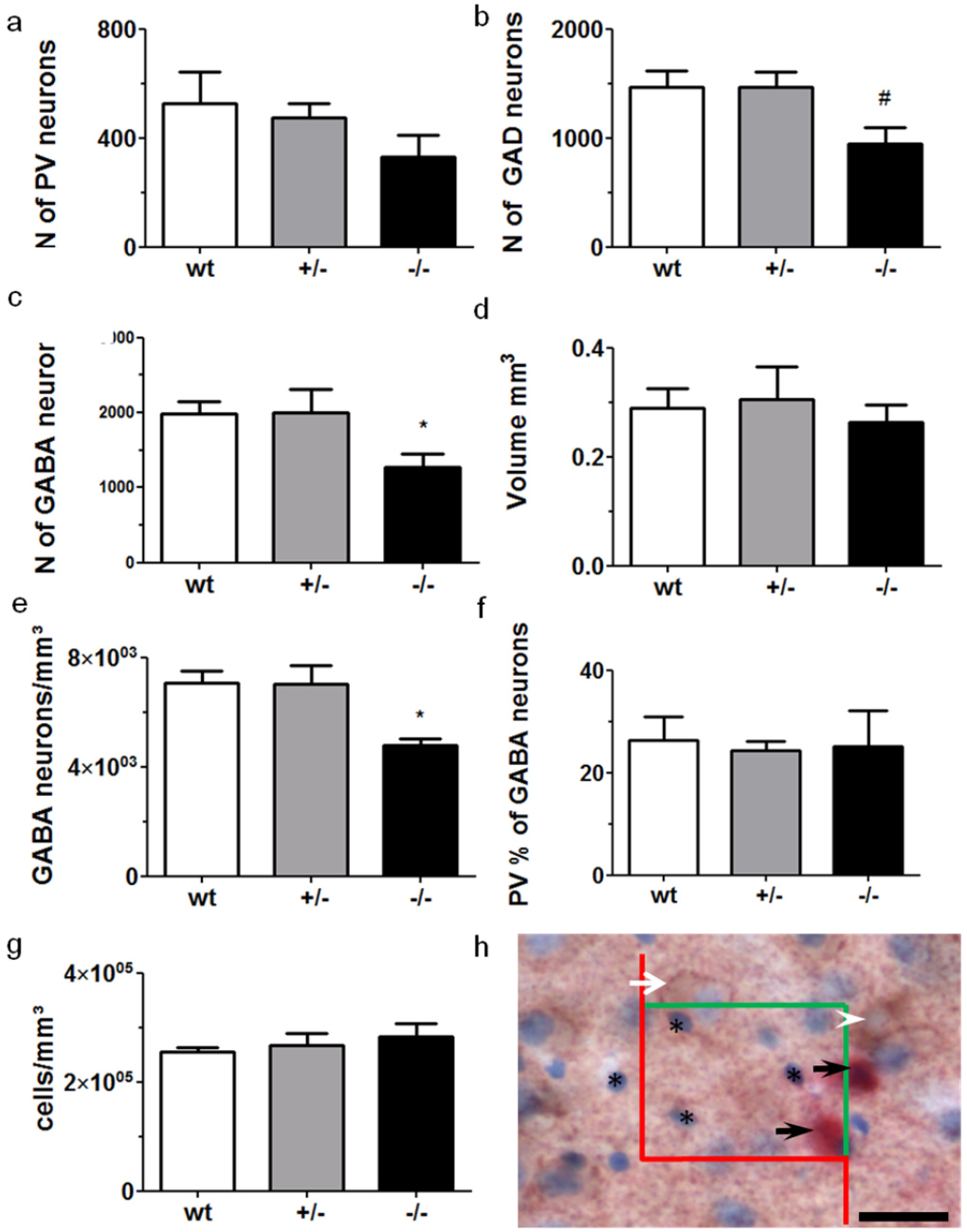

Fig.3-9 Stereological investigation of basolateral amygdaloidal complex (BLC) in *Tph2*$^{-/-}$ mice

Total number of PV neurons (a) and total number of GAD 65/67-specific neurons (b) were estimated in the BLC. These were summed up to the total number and total density of GABAergic neurons (c) and (e). The percentage of PV neurons among total GABAergic neurons is shown in (f). Total volume and total number of all cells of the BLC were counted by stereological estimates through optical dissectors of Nissl counterstaining (h). Higher resolution image in (h) indicates an optical dissector displayed on a Nissl counterstained double GAD/PV staining. White arrowheads indicate single labeled GAD 65/67-specific brown neurons. Black arrows show red PV neurons. Normal white arrows show somatic targets of GAD 65/67-specific fibers onto unstained cells. Stars indicate counted Nissl stained cell nuclei. Scale bar in h = 50 μm. Bars indicate mean ± SEM with N = 5. Kruskal-Wallis test followed by Dunn's test: # = $0.1 \geq p > 0.05$; * = $0.05 \geq p > 0.01$

3.5.2 GABAergic interneuron numbers in dorsal Hippocampus

The dorsal and ventral hippocampus represent functionally distinct structures (Fanselow and Dong, 2010). Because the numerical densities of GABAergic neurons were previously found to vary significantly between dorsal and ventral hippocampus (Jinno and Kosaka, 2006) we focused on the dorsal hippocampus. The different hippocampal layers were delineated in Nissl counterstained sections. After GAD/PV double labeling, GAD65/67 neurons were counted separately from PV neurons as in the BLC (Fig. 3-10).

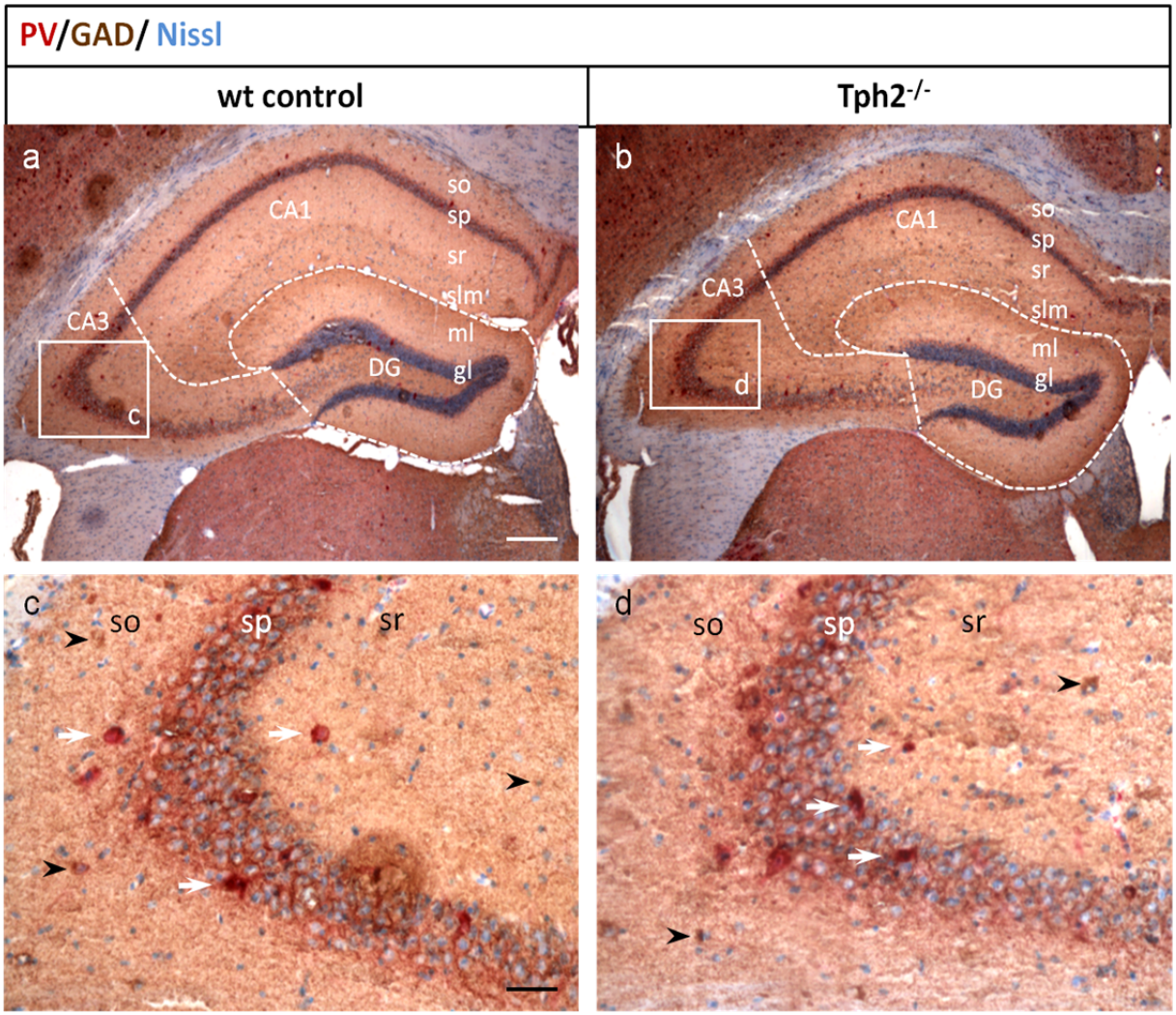

Fig.3-10 Parvalbumin (PV) and glutamic acid decarboxylase (GAD) 65/67 immunostaining in the dorsal Hippocampus.

Pictures (a) and (b) depict the dorsal hippocampus at –1.70 from bregma in *wt* and *Tph2*$^{-/-}$ animals. Higher resolution images are depicted in (c) and (d) of the CA3 region. Black arrowheads indicate single labeled GAD65/67 brown neurons. White arrows show red PV neurons. Arrowheads indicate single labeled GAD 65/67-specific brown neurons. Sharp arrows show red PV neurons. Normal white arrows show somatic targets of GAD 65/67-specific fibers onto unstained cells. Lines indicate the boundaries of the CA1, CA3, and dentate gyrus (DG). So, stratum oriens; sp, stratum pyramidale; sr, stratum radiatum; slm, stratum lacunosum moleculare; gl, glomerular layer; ml, molecular layer; h. hilus. Scale bar in a = 250 µm and in c = 50µm.

No significant differences between *Tph2*$^{-/-}$ mice and *wt* mice were detected in the different hippocampal cell layers including stratum lacunosum moleculare (slm), stratum radiatum (sr), stratum pyramidale (sp) and stratum oriens (so) (Fig. 3-11 i-j). However, by analyzing total CA1, CA3, and dentate gyrus (DG) regions separately, a trend towards reduced PV neurons in the CA3 region of *Tph2*$^{-/-}$ mice was found (p = 0.059), while no significant effects were detected in volumes (Fig. 3-11 g) and total GABAergic neurons (Fig. 3-11f,h) within these regions.

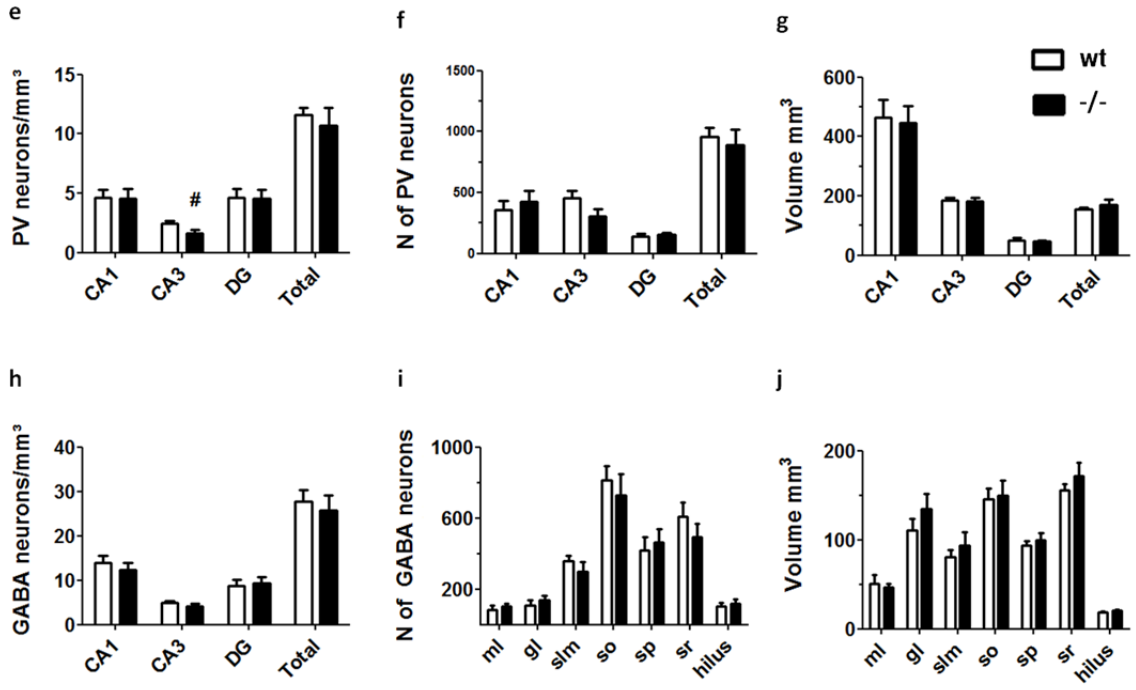

Fig. 3-11 Counting of dorsal hippocampal GABAergic neurons in *Tph2*$^{-/-}$ mice
Pictures (a) and (b) depict the dorsal hippocampus at –1.70 from bregma in *wt* and *Tph2*$^{-/-}$ animals. Higher resolution images are depicted in (c) and (d) of the CA3 region. Density of PV neurons (a), total number of GABAergic neurons (b), volumes (c) and densities (d) of GABAergic neurons were calculated in different regions of the dorsal hippocampus. Laminar distribution of GABAergic neurons are shown in (e) and volumes in (f) of all hippocampal layers.
So, stratum oriens; sp, stratum pyramidale; sr, stratum radiatum; slm, stratum lacunosum moleculare; gl, glomerular layer; ml, molecular layer; h. hilus. Graphs' bars indicate mean ± SEM with N = 6. Student's t-test: # = $0.1 \geq p > 0.05$; * = $0.05 \geq p > 0.01$

PV neurons within the total dorsal hippocampus accounted for 40% of total GABAergic neurons in *wt* and *Tph2*$^{-/-}$ mice (Fig. 3-13). Interestingly, the proportion of PV neurons in the hippocampus significantly differed between hippocampal regions ($H_{(3)} = 8.43$; $p = 0.015$; CA1 vs. CA3 and DG $p \leq 0.05$) only within *wt* controls but not in *Tph2*$^{-/-}$mice (Fig. 3-13)

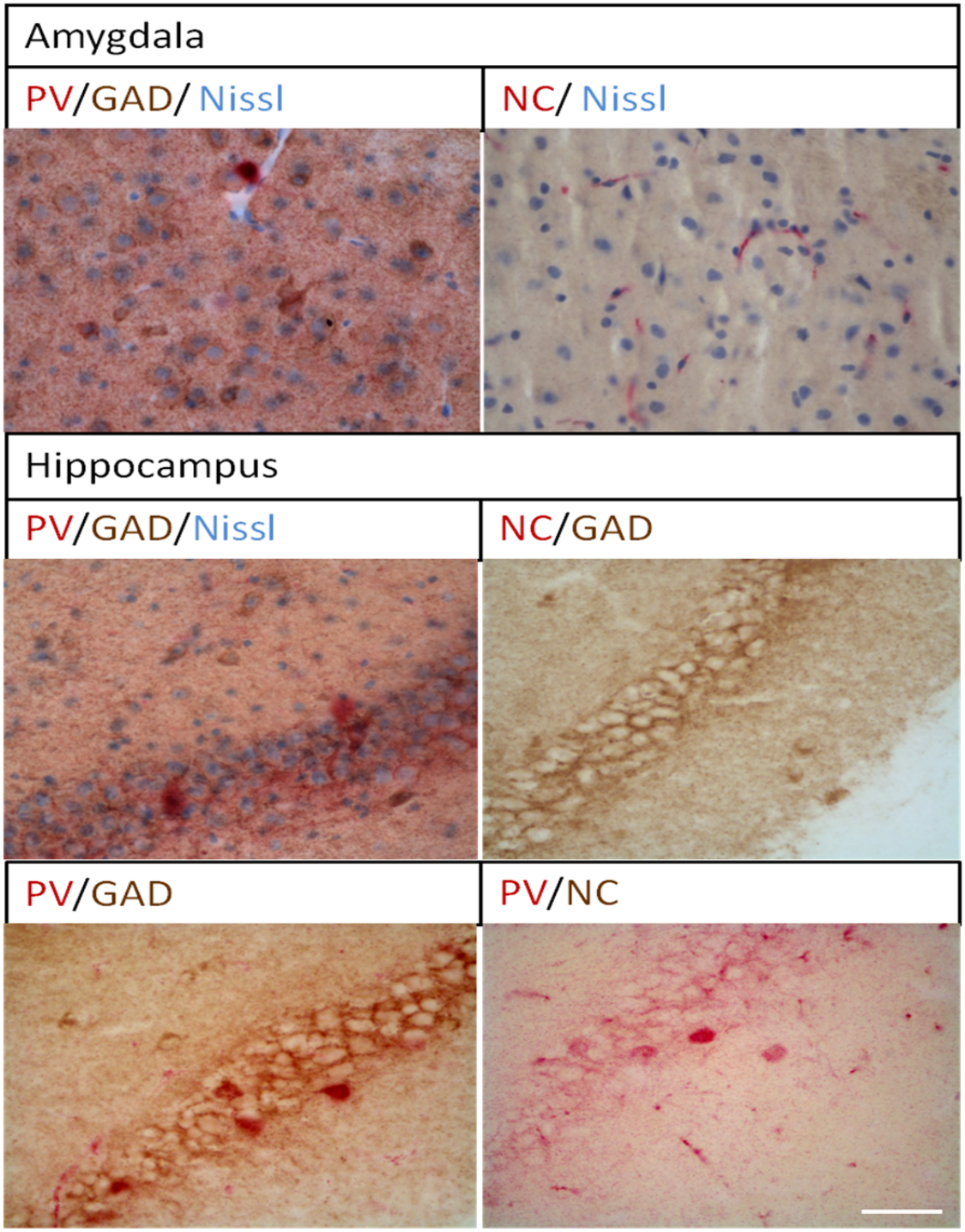

Fig.3-12 Negative controls of IHC double labeling of GAD 65/67 and Parvalbumin (PV) Double labeling of GAD 65/67 and PV in the amygdala (AMY) and negative control omitting both primary antibodies are shown in (a) and (b). Pictures (c-f) show the hippocampus with Nissl counterstained double labeling of GAD 65/67 and PV (c) and without Nissl counterstain in (e). Single stained sections omitting one of both primary antibodies in (d) and (f). Scale bar in b and h = 100 µm

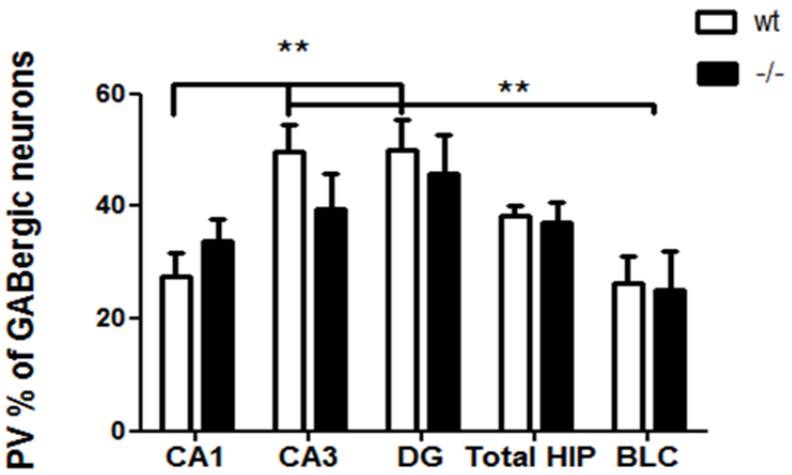

Fig. 3-13 Percentage of PV neurons among GABAergic neurons within the brain regions assessed.

BLC: basolateral complex of the amygdala; DG: dentate gyrus; Total HIP: total hippocampus. Bars indicate mean ± SEM with N = 6. Kruskal-Wallis followed by Dunn's test. * $p \leq 0.05$; ** = $p \leq 0.01$

3.6 Anxiety-like and depression-like behaviors in response to stress

Due to the complexity of 5-HT function within the different brain regions involved in emotion regulation a battery of behavioral tests was conducted to assess different phenotypes of emotional related behavior. In order to assess anxiety-like behavior we used the elevated plus maze (EPM) and the Open-field (OF). Unstressed *Tph2*$^{-/-}$ mice tended to spend less time in the closed arm than *wt* controls, although this was not significant ($F(2,21)= 0.60$, $p = 0.56$) Unstressed males also did not show differences in total distance traveled ($F(2,21)=2.58$, $p=0.102$;). However, CMS increased the total distance travelled ($F (1, 27) = 4.2$, $p=0.05$), in stressed *wt* ($F (1, 13) =7.43$, $p=0.017$) and stressed *Tph2*$^{-/-}$ mice. Interestingly, CMS increased the distance traveled in the closed arm for *wt* mice ($F (1, 13) =8.01$, $p=0.014$), whereas *Tph2*$^{-/-}$ mice were insensitive to CMS ($F (1, 14) =0.19$, $p=0.67$) and travelled longer distances in the closed arm of the EPM than stressed *wt* mice ($F (1, 13) =11.77$, $p=0.004$) (Fig. 3-14).

Additionally, *Tph2*$^{-/-}$ mice spent less time in the closed arm (F(1,27)=9.80, p=0.004) of the EPM. Stress specifically affected *wt* mice (F(1,27)=5.20, p=0.031), which spent more time in the closed arm than unstressed *wt* controls. In contrast *Tph2*$^{-/-}$ mice spent less time in the closed arm (F(1,13)=15.47, p=0.002) compared to *wt* controls and were not affected by CMS (F(1,14)=0.75, p=0.4, Fig. X?), while stressed *wt* controls spent significantly more time in the closed arm (F(1,13)=6.01, p=0.029) (Gutknecht et al., submitted)

To assess depression-like behavior in mice, the time spent floating, referred to as immobility time was measured as an index of behavioral despair in the Porsolt swim test. *Tph2*$^{-/-}$ mice exhibited significantly more immobility time (F (2, 42) =7.64, p=0.002) compared to *Tph2*$^{+/-}$ and *wt* mice. This was also observed for the latency to immobility (F (2, 42) =9.79; p<0.001). No significant differences were found between *Tph2*$^{+/-}$ and *wt* mice. As a test for anhedonia, the sucrose preference test was conducted at basal level before and after the behavioral battery. *Tph2*$^{-/-}$ mice showed increased sucrose intake compared to *Tph2*$^{+/-}$ and *wt* mice at basal level as well as after the stressful behavioral battery (Gutknecht et al., submitted).

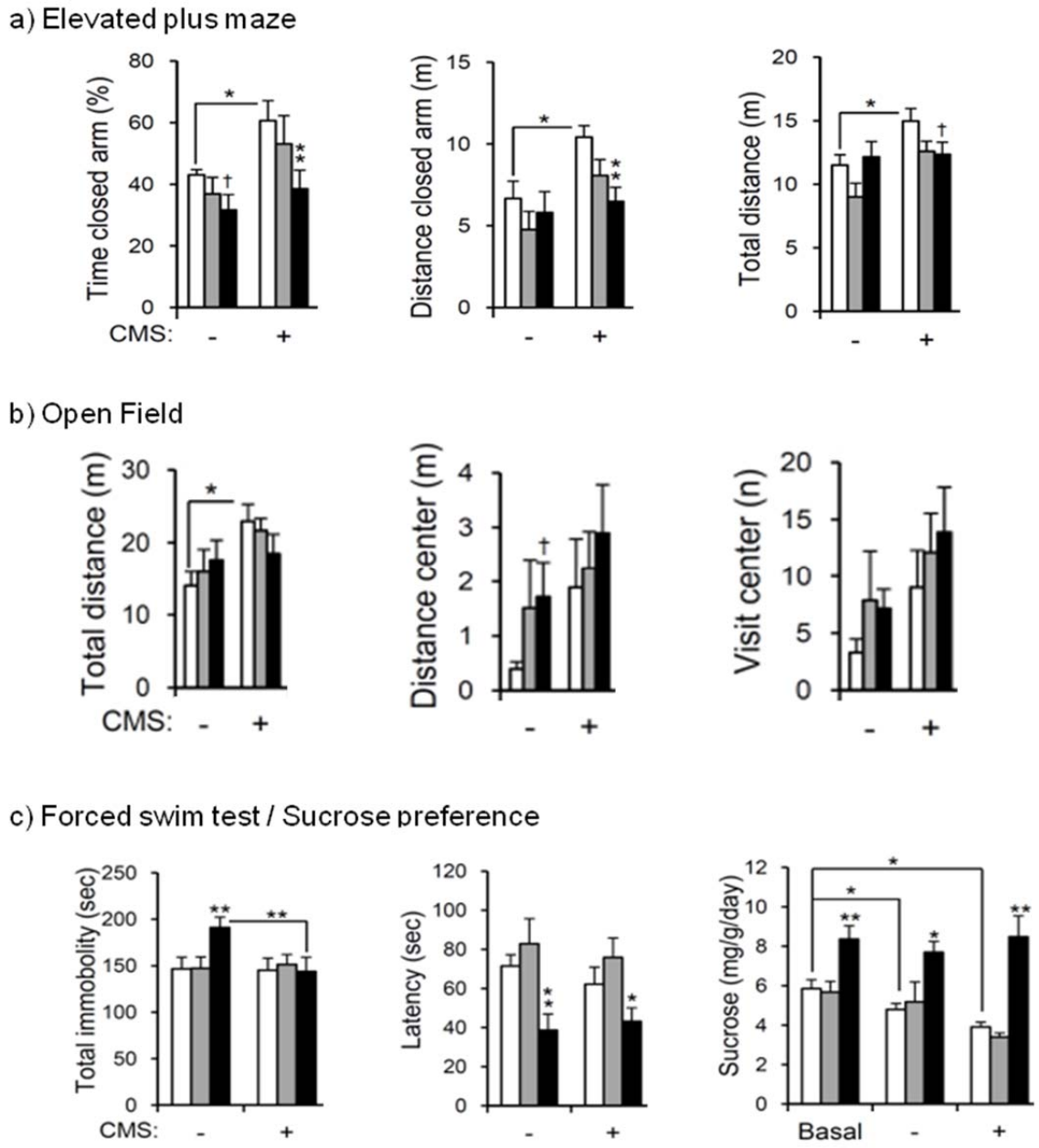

Fig. 3-14 Anxiety-like and depression-like behaviors in response to stress of *Tph2*$^{-/-}$ mice

Tph2$^{-/-}$, Tph$^{+/-}$ and *wt* male mice were tested in the elevated plus-maze (EPM) (a) and the open-field test (b) after 3 weeks of chronic mild stress (CMS) or undisturbed rearing. In the EPM test the total distance in all areas of an elevated plus maze (EPM), the percentage of time spent in the closed arm was assessed as measurements for anxiety-like behavior (a), in the open field exploratory activity were assessed by the total distance travelled, time spent in the center and the number of visits to the center. Data are presented as mean ± SEM; N=8; One-way ANOVA followed by Tuckey's post-hoc test: *p<0.05, **p<0.01, †0.05<p<0.1. (kindly provided by Dr. L. Gutknecht and S. Popp)

4. Discussion

5-HT as a neurotransmitter is a key modulator GABAergic and glutamatergic transmission. Its role as regulator of mood states has been investigated for decades and dysfunction of the serotonergic system provides a risk factor for psychiatric disorders. Given the high use of mouse models with targeted deletions of serotonergic genes in psychiatric disorders (for review see Lesch 2012) in the last decade, the *Tph2*$^{-/-}$ mouse line represents the first generation and characterization of a mouse model for complete 5-HT synthesis deficiency in the CNS. Although an important role of 5-HT has been proposed acting on brain development (Whitaker-Azmitia et al., 1996), *Tph2*$^{-/-}$ mice are viable but exhibit postponed development reflected by reduced body weight and size during the first four months (Alenina et al., 2009). With respect to the immense importance of 5-HT as a neurotransmitter in emotion regulation, it is intriguing that complete loss of 5-HT does not seem to restrict an individual as severe as an altered amount of 5-HT.

4.1 Alterations of the serotonergic system in Tph$^{-/-}$ mice

Generation, maintenance, migration and target projection pattern of 5-HT deficient raphe neurons do not appear to be impaired (Gutknecht et al., 2008) as demonstrated by immunohistochemistry against 5-HTT. A compensatory upregulation of Tph1 could be ruled out, as no Tph1 is expressed in *Tph2*$^{-/-}$ and *wt* mice as shown by IHC. Recent data indicate a fundamental role of the transcription factors *Pet-1* (Liu et al., 2010) and Lmx1b (Dai et al., 2008) in development and maintenance of the serotonergic phenotype during pre- and postnatal development into adulthood. However, density and expression patterns of *Pet-1* were not changed indicating a serotonergic system of *Tph2*$^{-/-}$ mice, which develops all determinants of the serotonergic phenotype besides *Tph2* and 5-HT.

This is supported by the expression of 5-HT1A receptors. These receptors are essential for normal functioning of the 5-HT system and their density is increased in target brain regions especially in the PFC and septum of *Tph2*$^{+/-}$ *Tph2*$^{-/-}$ and mice. This finding may be explained by a direct mechanism to compensate reduced 5-HT concentrations through increased expression of *5-htr1a* or reduced internalization of these receptors (Riad et al., 2004). In mice with increased 5-HT levels like 5-Htt$^{-/-}$ mice (Fabre et al., 2000) 5-HT1A and 1B heteroreceptors are reduced and desensitized in target brain regions. Thus, the Tph2$^{+/-}$ mice may represent a mirror phenotype to mice with increased 5-HT signaling.

Interestingly, the mean firing rate of serotonergic neurons in *Tph2*$^{-/-}$ mice is not affected *in-situ* (Gutknecht et al., under revision) providing further evidence of functional serotonergic neurons. This implicates that serotonergic neurons may fire properly although not releasing 5-HT and may signal through another substance. In fact monoaminergic neurons including 5-HT neurons have been shown to co-release glutamate (Trudeau, 2004) and neuroactive peptides (Hokfelt et al., 2000). Furthermore, autoinhibition through 5-HT1A receptors is disabled by lack of 5-HT, which may result in an increased firing rate of 5-HT neurons in *Tph2*$^{-/-}$ mice.

4.2 Fluorescence activated cell sorting of eGFP labeled 5-HT neurons

In order to identify factors, which impact on the survival and functioning of *Tph2* ablated 5-HT neurons I co-fostered the *Tph2*$^{-/-}$ mice with *Pet-1* Cre. eGFP mice. This resulted in strong eGFP expression in all formerly 5-HT positive neurons. Although some neurons exhibit a stronger eGFP signal, which might be caused by altered expression levels of *Pet-1* in different subsets of 5-HT neurons, virtually all eGFP neurons were Tph2 positive in the *wt* as well as in the knockout. This might be useful regarding the heterogeneity of the raphe nuclei and their specific function. Unfortunately, it was not possible to sort the respective eGFP

labeled 5-HT neurons by FACS in order to search for factors e.g. genes or proteins, which are responsible for their normal development and functioning. This may be due to several reasons including the small amount of 5-HT neurons at E17, the digestion of embryonic tissues or the long transportation time to the FACS. Rude FACS procedures may have caused cell death as well worsening already weak intrinsic expression of eGFP, which requires counterstaining with an anti-eGFP antibody to identify eGFP neurons properly. According to Wylie and coworkers(2010), it is possible to FACS sort eGFP labeled 5-HT neurons at embryonic day 14. Nevertheless, this might be possible due to another *Pet-1*-Cre eGFP line with enhanced eGFP expression in 5-HT neurons without the use of the Cre/loxP system, which may have an impact on cell viability.

4.3 High performance liquid chromatography (HPLC) measurements

4.3.1 Measurements of monoaminergic neurotransmitter

Tph2 inactivation resulted in a complete loss of 5-HT immunoreactivity. Nevertheless some remaining traces of 5-HT were detected by HPLC analysis in target brain regions like the amygdala and PFC. We speculate that the remaining 5-HT is due to contamination of the samples by blood, as 5-HT is stored in high concentration in erythrocytes (Côté et al., 2003) and released for vasoconstriction processes in case of an injury. Another cause of potential bias may be another substance with the same retention time as 5-HT. Furthermore, very low 5-HT levels were also detected in *Tph2*$^{-/-}$ mice (Alenina et al., 2009) as well as in *Tph1*/*Tph2* double knockout mice (Savelieva et al., 2008). Interestingly, dopamine and noradrenalin levels were affected by the absence of 5-HT in a genotype and brain region dependent manner, which may be due to the lack of 5-HT function through 5-HT receptors expressed on both monoaminergic systems (Mongeau et al., 1997, Navailles and De Deurwaerdere, 2011). Furthermore, dopamine concentrations were reduced in the amygdala. Similar results

although not significant were reported in *Tph2*$^{-/-}$ mice by two other studies (Savelieva et al., 2008, Alenina et al., 2009). All noradrenergic cells reside in the locus coeruleus (LC), a nucleus in the brainstem. 5-HT deficiency may downregulate noradrenalin concentrations within the LC. In fact, SSRIs stimulate tyrosine hydroxylase (TH) activity and may cause increased dopamine concentrations. Moreover, 5-HT/NE reuptake inhibitors (SNRI) represent potent drugs in the treatment of affective disorders (Sziray et al., 2007). The reduced norepinephrine concentrations are accompanied by a reduced number of TH positive cells were detected in LC subparts of *Tph2*$^{-/-}$ mice (Gutknecht et al., under revision). This points to a developmental effect of 5-HT on noradrenergic cells and might explain the reduced norepinephrine concentrations.

4.3.2 Differential regulated GABA and Glutamate concentrations in limbic brain regions

Tph2$^{-/-}$ mice are characterized by a lack of 5-HT synthesis from early prenatal development on, resulting in drastically reduced 5-HT concentrations in the adult brain. In comparison, *Tph2*$^{+/-}$ mice possess 20-30% reduced 5-HT concentrations in the rostral raphe but unaffected 5-HT concentrations in target brain regions of the 5-HT system, which might be explained by an increased activity of Tph2 within the target brain regions (Gutknecht et al., 2009). The neurotransmitter concentrations reported in this thesis represent the sum of intracellular as well as extracellular transmitters in one region. GABA concentrations are dependent on the activity of the GABA synthesizing enzymes GAD65 and GAD67 as well as on the activity of its degrading enzyme GABA-transaminase (GABA-T). GABA-T is highly saturated *in-vivo* (Behar et al., 1997). Therefore, the activity of both GAD isoforms, which is directly regulated by 5-HT through its receptors (Scott et al., 1997), is directly responsible for the total amount of GABA.

Here I could show that levels of GABA were specifically increased in the hippocampus of *Tph2*$^{-/-}$ mice, which clearly points to an important role of 5-HT regulating GABAergic transmission in the hippocampus. For example, beaded MnR 5-HT fibers with large spherical varicosities, and fine DR axons can be found in the dorsal hippocampus (Mamounas et al., 1991, Hensler, 2006). and selective activation of MnR 5-HT neurons was shown to activate dorsal hippocampal GABAergic neurons by 5-HT/Glutamate co-transmission (Varga et al., 2009) resulting in an overall inhibition of the hippocampal networks. However, 5-HT fibers, which predominantly innervate CB positive interneurons and VIP/CCK positive basket cells, which are activated by fast synaptic transmission via the 5-HT3 receptor, avoid PV neurons in the hippocampus (Gulyas et al., 1999). Thus lack of 5-HT may prevent the activation of GABAergic neurons in the hippocampus but the PV neurons may still be activated via cholinergic afferences (Lawrence, 2008). Thus, lack of 5-HT signaling in *Tph2*$^{-/-}$ mice may result in an increased cholinergic influence, which has been shown to act in an endocannabinoid system independent way depending on the fast-spiking PV neuron population (Cea-del Rio et al., 2010, Szabo et al., 2010) and may account for increased GABA concentration within the hippocampus of Tph2$^{-/-}$ mice. In addition to the lack of inhibitory GABAergic input, perisomatic inhibition of glutamatergic pyramidal neurons through 5-HT is also prevented in *Tph2*$^{-/-}$ mice (Gulyas et al., 1999). Thus, hippocampal glutamatergic projections neurons may be hyperaroused in *Tph2*$^{-/-}$ mice.

In contrast GABA concentrations in the PFC of *Tph2*$^{-/-}$ mice compared to *wt* controls remain unaffected by complete lack of 5-HT, whereas they are reduced specifically in *Tph2*$^{+/-}$ mice . In general, 5-HT signaling reduces GABA release in the cortex (Kruglikov & Rudy, 2008).In fact, 5-HT1A receptors are expressed by fast-spiking GABAergic PV neurons (FSi) and on principal glutamatergic neurons. Their activation through 5-HT results in an overall inhibition of FSi activity and pyramidal activity Additionally, 5-HT2A receptors are expressed by the same FSi populations and the apical dendrites in the PFC and the interplay between these two

5-HT receptors seems to be responsible for the regulation of slow wave gamma oscillations (Puig et al., 2010). Because 5-HT1A receptors are upregulated in the PFC of *Tph2*$^{+/-}$ and *Tph2*$^{-/-}$ mice decreased GABA concentrations in the PFC of *Tph2*$^{+/-}$ mice as shown in this thesis may be the result of increased density and activation of 5-HT1A receptors (Gutknecht et al., under revision). In contrast to *Tph2*$^{+/-}$mice, enhanced 5-HT1A receptors of *Tph2*$^{-/-}$ mice will not be activated due to the lack of 5-HT, which might explain the unaffected concentrations of GABA detected in *Tph2*$^{-/-}$ mice within this study. Furthermore, I could show that GABA concentrations were the reverse in the amygdala compared to the PFC. In contrast to the inhibition of GABAergic cells in the cortex by 5-HT1A receptors, GABAergic cells in the amygdala may be more activated through 5-HT2A and 2C receptors (Jiang et al., 2009). Here these receptors are expressed on different GABAergic subpopulations (Hale et al., 2010) and strongly inhibit Glutamatergic output neurons. Thus, due to lack of inhibition, lack of 5-HT in *Tph2*$^{-/-}$ mice would result in a total hyper-arousal of the amygdala following emotional stimuli. According to Pape and Paré (2010), this process might be counterbalanced by direct glutamatergic influence of the prelimbic and infralimbic PFC on the BLC by increasing the frequency of inhibitory postsynaptic potentials in basolateral output neurons. This is indicated by increased glutamate concentrations in the PFC as well as unaffected GABA and glutamate concentrations in the amygdala of *Tph2*$^{-/-}$ mice. On the other hand, GABA concentrations of *Tph2*$^{+/-}$ were increased in the amygdala compared to *wt* control mice whereas glutamate concentrations were not affected. This points to an increased activation of GABAergic neurons, most likely through increased activation of 5-HT2A/C receptors. This finding is in line with processes occurring in homozygous R439H *TPH2* knockin mice. These mice carrying a humanized single nucleotide polymorphism (SNP), display more than 50% reduced 5-HT concentrations throughout brain regions and were found to display increased 5-HT2A receptor expression in the PFC (Jacobsen et al., 2011). Nevertheless, glutamate is increased slightly in the PFC of *Tph2*$^{-/-}$ mice in a genotype dependent manner but not in

amygdala and hippocampus. Thus, .other neurotransmitter systems like dopamine or noradrenalin have been shown to influence limbic brain regions as well (d'Onofrio et al., 1997, Duve et al., 1997) and may act in concert with the above mentioned receptor functions to regulate GABA and glutamate function in *Tph2*$^{+/-}$ and *Tph2*$^{-/-}$ mice.

4.4 Developmental effect of 5-HT deficiency on GABAergic neurons in limbic brain regions

Besides the regulation of both GAD isoforms, another explanation for altered GABA concentration in the tissue may be developmental mechanisms affecting the number of GABAergic neurons. In contrast to its function in adult stages, 5-HT plays an important role during early pre-natal and post-natal stages (Gaspar et al., 2003, Côté et al., 2007). Interestingly, projection patterns of 5-HT fibers do not seem to be affected in *Tph2*$^{-/-}$ mice (Gutknecht et al., under revision). However, alterations in 5-HT functioning affect GABAergic cell migration (Vitalis et al., 2007, Riccio et al., 2009). A potential mechanism responsible for the changes in GABA concentrations between *Tph2* genotypes may be an altered migration of GABAergic precursors, which leads to a reduced number of GABAergic neurons.. However, the results show that remaining 5-HT in Tph2$^{+/-}$ mice is sufficient to develop normal numbers of GAD65/67-specific neurons within the BLC of *Tph2*$^{+/-}$ mice. Interestingly, in this thesis GAD65/67-specific neurons in the BLC of *Tph2*$^{-/-}$ mice were reduced, which seemed to be influenced by PV-specific neurons. Virtually all PV-specific neurons have been shown to be GABAergic in the BLC of mice (Gulyas and Roland, 1994) and rats (McDonald and Mascagni, 2001). According to our findings PV-specific cell numbers account for more than 25% of GABAergic cells in the BLC although their reduction itself did not reach significance due to the small sample size. Thus, other GABAergic neuron subpopulations might account for the decreased density of GABAergic neurons as well (Vitalis et al., 2007, Spampanato et al., 2011). Furthermore, since total cell numbers in the

BLC remain unchanged, other cell populations like glial cells or glutamatergic neurons within the BLC may be increased, which may explain unaffected total cell numbers. In contrast to our findings in the BLC *Tph2*$^{-/-}$ and *wt* mice in the hippocampus displayed a trend to reduced PV-specific neuron numbers specifically in the CA3 region of the dorsal hippocampus. However, no difference between GABAergic cell numbers in the different layers and no difference by analyzing the total hippocampus was found. Nevertheless, migration of GABAergic neurons into the amygdala and hippocampus during pre- and early post-natal development (Kalaska et al., 1997) appears to precede the expression of 5-HT1A/2A receptors, which might be transiently expressed during migration processes (Hurley et al., 1997). Additionally, within the cortex, 5-HT6 receptors expressed on developing and migrating GABAergic neurons control their migratory speed (Riccio et al., 2009). Albeit yet speculatively, these findings may indicate mechanisms during development to cope with a lack of 5-HT through altered integration of GABAergic interneuron into limbic networks.

Further studies will need to clarify the functional relevance of decreased GABAergic neuron numbers, which are rather subtle in the dorsal hippocampus compared to the strong effect on GABA concentrations. In summary, it may be possible that developmental changes of GABAergic cell numbers caused by a 5-HT deficiency during development are partly responsible for the alterations in neurotransmitter metabolism of *Tph2*$^{-/-}$ mice in adulthood.

4.5 Implications on anxiety-like behavior

Anxiety of an animal is a complex emotional state based on a conflict of approach and avoidance behaviors in unpredictable situations (Walker et al., 2003). Based on pharmacological findings Graeff and Zangrossi proposed a dual role of 5-HT to modulate different defensive behaviors via activation of distinct 5-HT receptors expressed on target neurons (2010). In line with this hypothesis, the current study linked developmental processes

impacting on GABAergic neuron populations in the hippocampus (Danglot et al., 2006) and the amygdala (Soma et al., 2009) to an overall decreased innate anxiety phenotype. Fear and anxiety can be distinguished as the following: fear is an adaptive state of apprehension that begins rapidly and dissipates quickly once the threat is removed, which is also called „phasic fear“ (Davis and Shi, 2000). In contrast to fear, anxiety is proposed to be elicited by less specific and less predictable threats, or by those that are physically or psychologically more distant (Walker et al., 2009). Thus, anxiety is a more long-lasting state of apprehension also called „sustained fear“ (Davis and Shi, 2000). In behavioral paradigms, the open-field or EPM is used to test sustained fear, which is called from now on innate anxiety. Innate anxiety seems to involve increased synchronized theta activity between the ventral hippocampus and the PFC (Liu and Scott, 1997). This synchronized activity by theta frequencies between limbic brain regions may be involved in the control of fear memory retrieval and extinction (Seidenbecher et al., 2003, Lesting et al., 2011b). Important for synchronous oscillatory activity within PFC, amygdala, and hippocampus are GABAergic interneurons, which are regulated by 5-HT through specific receptors (Klausberger, 2009, Puig et al., 2010, Lesting et al., 2011a).

Here we show that *Tph2*$^{-/-}$ mice exhibit an altered anxiety-related phenotype with a dissociation of innate anxiety-like behavior indicated by less time spent in the closed arm of the EPM and an increase in conditioned fear learning (Gutknecht et al., submitted). Contradictory, *Tph2*$^{+/-}$ mice display an intermediate anxiety-like behavioral phenotype compared to *Tph2*$^{-/-}$ and *wt* animals. So far, the PFC has been considered to be involved in emotion regulation by integrating sensory and contextual information from the hippocampus to regulate downstream subcortical brain regions of the limbic system, like the amygdala (Del Arco and Mora, 2009). which mediate downstream behavioral responses (Rogers et al., 1997, Holmes, 2008). Here, glutamate levels in the PFC, which were found to be increased in a genotype-dependent manner in *Tph2*$^{+/-}$ and *Tph2*$^{-/-}$ mice, may reflect the potential of the PFC

to control emotional responses via intercalated neurons (ITC) situated at the border between BLC and central nucleus of the amygdala (Jungling et al., 2008). Thus, the differential regulated GABA concentrations may point to an increased activity of glutamatergic projection neurons of the PFC blocking the activation of GABAergic neurons in the central amygdala of *Tph2*$^{-/-}$ mice, which seem to result in normalized concentrations of GABA. Nevertheless the underlying regulatory mechanisms responsible for the behavioral phenotype of *Tph*$^{+/-}$ and *Tph*$^{-/-}$ mice remains to be elucidated as well as the contribution of other limbic structures in the modulation of these behavioral responses e.g. the bed nucleus of the stria terminalis (BNST) (Davis et al., 2010).

4.6 5-HT deficiency induces depressive-like behavior which is rescued by CMS

In the forced swim test (FST) also called Porsolt test (Thomas et al., 1997) *Tph2*$^{-/-}$ mice showed increased time of total immobility as well as a shorter latency to float. This is an index of increased behavioral despair, which represents a possible cause for the development of depression in humans (Duman, 2010).

Whereas discrepant results between FST and TST were reported in *Tph2*$^{-/-}$ mice (Savelieva et al., 2008), we show here that the depression-like behavior in *Tph2*$^{-/-}$ mice is rescued by CMS, which is unlikely to be due to a stress-induced locomotor activation or higher impulsivity, since an increase was not recorded in the OF and EPM tests. Thus, CMS seem to rescue an increase in behavioral despair in 5-HT deficient mice by increasing resilience to the negative effects of *Tph2* inactivation (Gutknecht et al., under revision). This is in line with previous studies on PCPA treated rats, which experienced CMS (Harro et al., 2001).

In contrast to the depressive-like behavior *Tph2*$^{-/-}$ are insensitive to stress regarding their innate anxiety phenotype compared *wt* mice.

Especially inescapable stress like in the forced swim test or fear conditioning paradigms may activate 5-HT release of a different subset of 5-HT neurons than escapable (controllable) stress occurring in the OF or EPM (Maier and Watkins, 2005, Baratta et al., 2009). This might explain the intensified CMS effect on *wt* mice in the EPM and OF, which was not observable in the FST. Interestingly, in *Tph2*$^{-/-}$ mice this intensifying effect was prevented due to the lack of 5-HT, which indicates that 5-HT is important in mediating a normal innate anxiety-like behavior under CMS conditions.

4.7 Implications for emotion regulation

The previous sections have outlined how 5-HT deficiency effects the development and neurochemistry of the GABAergic system in *Tph2*$^{-/-}$ mice and how loss of 5-HT impacts on emotion related behavior in combination with CMS. In the following, the presented results will be set into a more global context to explain the regulation of emotional behavior by 5-HT. According to the dual 5-HT hypothesis by Graeff and coworkers (2010), distinct target regions of neural circuits emerging from the DR and MnR are involved in different forms of anxiety. On the one hand, the defensive avoidance system operates while leaving a dangerous situation (active avoidance) and is expressed in specific forms of fear. Whereas on the other hand the defensive approach system is active while entering a dangerous situation (e.g. cautious 'risk assessment' approach behavior) or withholding entrance (passive avoidance), which is anxiety (McNaughton and Corr, 2004). 5-HT and noradrenalin are involved in the regulation of these behaviors and seem to integrate environmental factors like stress.

Nevertheless, *Tph2*$^{-/-}$ mice exhibit a dissociation of the anxiety-related phenotype with a decrease of innate anxiety-like behavior and an increase in conditioned fear responses (Gutknecht et al., submitted). This dissociation seems to set the basis for an altered response

to stress. These results suggest that 5-HT acts through distinct receptors on the development and migration of GABAergic networks in limbic brain regions. In combination with altered activity of distinct 5-HT receptors expressed on different sets of GABAergic interneurons and increased influence of other neurotransmitter systems in adulthood, the alteration in GABAergic neuron populations may be responsible for an altered anxiety and depressive-like behavior. Still further research is required to reveal whether other GABAergic subpopulations are affected as well. In addition, it needs to be explored which 5-HT receptors mediate the migration of GABAergic neurons in *Tph2*$^{-/-}$ mice and how this impacts the functionality of circuits involved in the regulation of emotional behavior. However, due to the importance of the 5-HT system in regulating an adequate response to threatening and stressful situations, it remains to be clarified whether mice exhibiting brain 5-HT deficiency react appropriately in more naturalistic environments.

To disentangle the function of 5-HT in these complex neuronal networks and regulations further mouse models like the *Tph2*$^{-/-}$ mouse are needed to model basic mechanisms operating in human disorders of emotion dysregulation.

5. Summary

Based on genetic association and functional imaging studies, reduced function of tryptophan hydroxylase-2 (TPH2) has been shown to be critically involved in the pathophysiology of anxiety-disorders and depression. In order to elucidate the impact of a complete neuronal 5-HT deficiency, mice with a targeted inactivation of the gene encoding *Tph2* were generated. Interestingly, survival of *Tph2*$^{-/-}$ mice, the formation of serotonergic neurons and the pathfinding of their projections was not impaired. Within this thesis, I investigated the influence of 5-HT deficiency on the γ-amino butyric acid (GABA) system. The GABAergic system is implicated in the pathophysiology of anxiety disorders. Therefore, measurement of GABA concentrations in different limbic brain regions was carried out. These measurements were combined with immunohistochemical estimation of GABAergic cell subpopulations in the dorsal hippocampus and amygdala.

In *Tph2*$^{-/-}$ mice GABA concentrations were increased exclusively in the dorsal hippocampus. In heterozygous *Tph2*$^{+/-}$ mice concentrations of GABA were increased in the amygdala compared to *Tph2*$^{-/-}$ and *wt* control mice, while the reverse was found in the prefrontal cortex. The changes in GABA concentrations were accompanied by altered cell density of GABAergic neurons within the basolateral complex of the amygdala and parvalbumin (PV) neurons of the dorsal hippocampus and by adaptational changes of 5-HT receptors. Thus, adaptive changes during the development on the GABA system may reflect altered anxiety-like and depressive-like behavior in adulthood. Moreover, chronic mild stress (CMS) rescues the depressive-like effects induced by 5-HT deficiency. In contrast, 5-HT is important in mediating an increased innate anxiety-like behavior under CMS conditions. This is in line with a proposed dual role of 5-HT acting through different mechanisms on anxiety and depressive-like behavior, which is influenced by gene-environment interaction effects. Further research is needed to disentangle these complex networks in the future.

6. Zusammenfassung

Genomweite Assoziationsstudien in Kombination mit bildgebenden Studien zeigten, dass eine verringerte Funktion der Tryptophanhydroxylase-2 (*Tph2*) eine zentrale Rolle in der Pathophysiologie von Angststörungen und Depression spielt. Jedoch sind die einer Angststörung oder Depression zugrundeliegenden genauen Mechanismen noch nicht verstanden. Um den Einfluss einer 5-HT Defizienz zu untersuchen, wurden *Tph2* ablatierte ($Tph2^{-/-}$) Mäuse mittels zielgerichteter Mutagenese generiert. Der Verlust des *Tph2* Gens hatte interessanterweise keinen Einfluss auf die Entwicklung vormals serotonerger Neurone und das Überleben der Tiere. In vorherigen Untersuchungen konnte gezeigt werden, dass 5-HT das GABAerge System, welches in der Pathophysiologie von Angststörungen eine zentrale Rolle spielt, in seiner Entwicklung beeinflusst. Daher wurden im Rahmen dieser Arbeit in verschiedenen Gehirnregionen des limbischen Systems Konzentrationen von GABA gemessen. Außerdem wurden mittels immunhistologischer Untersuchungen die Auswirkungen einer 5-HT Defizienz auf GABAerge Neuronenpopulationen hin untersucht. In $Tph2^{-/-}$ Mäusen wurden erhöhte Konzentrationen im Vergleich zu $Tph2^{+/-}$ und *wt* Kontrollen von GABA im Hippocampus festgestellt. In der Amygdala zeigten die $Tph2^{+/-}$ Mäuse dagegen eine erhöhte Konzentration von GABA. Dieser Effekt auf $Tph2^{+/-}$ Mäuse war umgekehrt im PFC Kortex zu finden, der erniedrigte GABA Konzentrationen in $Tph2^{+/-}$ aufwies. Die Veränderungen auf der neurochemischen Ebene wurden begleitet von veränderten GABAergen Zelldichten im basolateralen Komplex der Amygdala und parvalbuminergen GABAergen Neuronen in der CA3 Region des dorsalen hippocampus. Zudem waren 5-HT1A Rezeptoren und ihre Signalwege hochreguliert.

Es scheint, dass der Verlust von 5-HT adaptive Veränderungen in der Entwicklung auf das GABAerge System zur Folge hat und die Basis für verändertes angstähnliches und depressionsähnliches Verhalten im Erwachsenenalter darstellt. Zusätzlich scheint eine 5-HT

Defizienz den depressiven Phänotyp im Porsolt Test auszugleichen. Demgegenüber scheint 5-HT wichtig für ein erhöhtes angstähnliches Verhalten unter CMS Bedingungen zu sein. Dies unterstützt die Hypothese einer Doppelrolle von 5-HT innerhalb von Signalwegen und Mechanismen des angst- und depressionsähnlichem Verhalten, die durch Umweltfaktoren wie Stress stark beeinflusst werden. Um den Patienten noch besser helfen zu können erfordert dies in der Zukunft weiterhin eine fundierte Entschlüsselung der dahinter verborgenen Mechanismen.

7. References

Alenina N, Kikic D, Todiras M, Mosienko V, Qadri F, Plehm R, Boye P, Vilianovitch L, Sohr R, Tenner K, Hortnagl H, Bader M (2009) Growth retardation and altered autonomic control in mice lacking brain serotonin. Proc Natl Acad Sci U S A 106:10332-10337.

Azmitia EC, Whitaker-Azmitia PM (1991) Awakening the sleeping giant: anatomy and plasticity of the brain serotonergic system. J Clin Psychiatry 52 Suppl:4-16.

Baehne CG, Ehlis AC, Plichta MM, Conzelmann A, Pauli P, Jacob C, Gutknecht L, Lesch KP, Fallgatter AJ (2009) Tph2 gene variants modulate response control processes in adult ADHD patients and healthy individuals. Mol Psychiatry 14:1032-1039.

Baratta MV, Zarza CM, Gomez DM, Campeau S, Watkins LR, Maier SF (2009) Selective activation of dorsal raphe nucleus-projecting neurons in the ventral medial prefrontal cortex by controllable stress. Eur J Neurosci 30:1111-1116.

Behar TN, Dugich-Djordjevic MM, Li YX, Ma W, Somogyi R, Wen X, Brown E, Scott C, McKay RD, Barker JL (1997) Neurotrophins stimulate chemotaxis of embryonic cortical neurons. Eur J Neurosci 9:2561-2570.

Berger M, Gray JA, Roth BL (2009) The Expanded Biology of Serotonin. Annual Review of Medicine 60:355-366.

Bombardi C (2011) Distribution of 5-HT2A receptor immunoreactivity in the rat amygdaloid complex and colocalization with gamma-aminobutyric acid. Brain Res 1370:112-128.

Bonn M, Schmitt A, Lesch KP, Van Bockstaele EJ, Asan E (2012) Serotonergic innervation and serotonin receptor expression of NPY-producing neurons in the rat lateral and basolateral amygdaloid nuclei. Brain Struct Funct.

Bonnin A, Torii M, Wang L, Rakic P, Levitt P (2007) Serotonin modulates the response of embryonic thalamocortical axons to netrin-1. Nat Neurosci 10:588-597.

Brown P, Molliver ME (2000) Dual serotonin (5-HT) projections to the nucleus accumbens core and shell: relation of the 5-HT transporter to amphetamine-induced neurotoxicity. J Neurosci 20:1952-1963.

Brown SM, Peet E, Manuck SB, Williamson DE, Dahl RE, Ferrell RE, Hariri AR (2005) A regulatory variant of the human tryptophan hydroxylase-2 gene biases amygdala reactivity. Mol Psychiatry 10:884-888, 805.

Canli T, Congdon E, Gutknecht L, Constable RT, Lesch KP (2005) Amygdala responsiveness is modulated by tryptophan hydroxylase-2 gene variation. J Neural Transm 112:1479-1485.

Canli T, Congdon E, Todd Constable R, Lesch KP (2008) Additive effects of serotonin transporter and tryptophan hydroxylase-2 gene variation on neural correlates of affective processing. Biol Psychol.

Canli T, Lesch KP (2007) Long story short: the serotonin transporter in emotion regulation and social cognition. Nat Neurosci 10:1103-1109.

Cea-del Rio CA, Lawrence JJ, Tricoire L, Erdelyi F, Szabo G, McBain CJ (2010) M3 muscarinic acetylcholine receptor expression confers differential cholinergic modulation to neurochemically distinct hippocampal basket cell subtypes. J Neurosci 30:6011-6024.

Chen GL, Vallender EJ, Miller GM (2008) Functional characterization of the human TPH2 5' regulatory region: untranslated region and polymorphisms modulate gene expression in vitro. Hum Genet 122:645-657.

Chowdhury N, Quinn JJ, Fanselow MS (2005) Dorsal hippocampus involvement in trace fear conditioning with long, but not short, trace intervals in mice. Behav Neurosci 119:1396-1402.

Cichon S, Winge I, Mattheisen M, Georgi A, Karpushova A, Freudenberg J, Freudenberg-Hua Y, Babadjanova G, Van Den Bogaert A, Abramova LI, Kapiletti S, Knappskog PM, McKinney J, Maier W, Jamra RA, Schulze TG, Schumacher J, Propping P, Rietschel M, Haavik J, Nothen MM (2008) Brain-specific tryptophan hydroxylase 2 (TPH2): a functional Pro206Ser substitution and variation in the 5'-region are associated with bipolar affective disorder. Hum Mol Genet 17:87-97.

Cordes SP (2005) Molecular genetics of the early development of hindbrain serotonergic neurons. Clin Genet 68:487-494.

Côté F, Fligny C, Bayard E, Launay JM, Gershon MD, Mallet J, Vodjdani G (2007) Maternal serotonin is crucial for murine embryonic development. Proc Natl Acad Sci U S A 104:329-334.

Côté F, Thevenot E, Fligny C, Fromes Y, Darmon M, Ripoche MA, Bayard E, Hanoun N, Saurini F, Lechat P, Dandolo L, Hamon M, Mallet J, Vodjdani G (2003) Disruption of the nonneuronal tph1 gene demonstrates the importance of peripheral serotonin in cardiac function. Proc Natl Acad Sci U S A 100:13525-13530.

d'Onofrio G, Kim YR, Schulze S, Lorentz T, Dorner K, Goossens W, Zini G, Tommasi M, Kendall R, Scott CS (1997) Evaluation of the Abbott Cell Dyn 4000 automated fluorescent reticulocyte measurements: comparison with manual, FACScan and Sysmex R1000 methods. Clin Lab Haematol 19:253-260.

Dai JX, Han HL, Tian M, Cao J, Xiu JB, Song NN, Huang Y, Xu TL, Ding YQ, Xu L (2008) Enhanced contextual fear memory in central serotonin-deficient mice. Proc Natl Acad Sci U S A 105:11981-11986.

Danglot L, Triller A, Marty S (2006) The development of hippocampal interneurons in rodents. Hippocampus 16:1032-1060.

Davila JC, Olmos L, Legaz I, Medina L, Guirado S, Real MA (2008) Dynamic patterns of colocalization of calbindin, parvalbumin and GABA in subpopulations of mouse basolateral amygdalar cells during development. J Chem Neuroanat 35:67-76.

Davis M, Shi C (2000) The amygdala. Curr Biol 10:R131.

Davis M, Walker DL, Miles L, Grillon C (2010) Phasic vs sustained fear in rats and humans: role of the extended amygdala in fear vs anxiety. Neuropsychopharmacology 35:105-135.

Deakin JF, Graeff FG (1991) 5-HT and mechanisms of defence. J Psychopharmacol 5:305-315.

Del Arco A, Mora F (2009) Neurotransmitters and prefrontal cortex-limbic system interactions: implications for plasticity and psychiatric disorders. J Neural Transm 116:941-952.

Di Pino G, Moessner R, Lesch P, Lauder J, Persico A (2004) Roles for serotonin in neurodevelopment: more than just neural transmission. Curr Neuropharmacol 2 403-418.

Duman CH (2010) Models of depression. Vitam Horm 82:1-21.

Duve H, Johnsen AH, Maestro JL, Scott AG, Jaros PP, Thorpe A (1997) Isolation and identification of multiple neuropeptides of the allatostatin superfamily in the shore crab Carcinus maenas. Eur J Biochem 250:727-734.

Fabre V, Beaufour C, Evrard A, Rioux A, Hanoun N, Lesch KP, Murphy DL, Lanfumey L, Hamon M, Martres MP (2000) Altered expression and functions of serotonin 5-HT1A and 5-HT1B receptors in knock-out mice lacking the 5-HT transporter. Eur J Neurosci 12:2299-2310.

Fanselow MS, Dong HW (2010) Are the dorsal and ventral hippocampus functionally distinct structures? Neuron 65:7-19.

Fendt M, Fanselow MS, Koch M (2005) Lesions of the dorsal hippocampus block trace fear conditioned potentiation of startle. Behav Neurosci 119:834-838.

Franklin KBJ, Paxinos G (1997) The mouse brain in stereotaxic coordinates. San Diego: Academic Press.

Gaspar P, Cases O, Maroteaux L (2003) The developmental role of serotonin: news from mouse molecular genetics. Nat Rev Neurosci 4:1002-1012.

Graeff FG, Guimaraes FS, De Andrade TG, Deakin JF (1996) Role of 5-HT in stress, anxiety, and depression. Pharmacol Biochem Behav 54:129-141.

Gulyas AI, Acsady L, Freund TF (1999) Structural basis of the cholinergic and serotonergic modulation of GABAergic neurons in the hippocampus. Neurochem Int 34:359-372.

Gulyas B, Roland PE (1994) Binocular disparity discrimination in human cerebral cortex: functional anatomy by positron emission tomography. Proc Natl Acad Sci U S A 91:1239-1243.

Gundersen HJ, Bagger P, Bendtsen TF, Evans SM, Korbo L, Marcussen N, Moller A, Nielsen K, Nyengaard JR, Pakkenberg B, et al. (1988) The new stereological tools: disector, fractionator, nucleator and point sampled intercepts and their use in pathological research and diagnosis. APMIS : acta pathologica, microbiologica, et immunologica Scandinavica 96:857-881.

Gutknecht L, Araragi N, Merker S, Waider J, Sommerlandt F, Mlinar B, Baccini G, Mayer U, Proft F, Hamon M, Schmitt A, Corradetti R, Lanfumey L, Lesch K (under revision) Impacts of Brain serotonin deficiency following Tph2 inactivation on development and raphe neuron serotonergic specification. PlosOne under revision

Gutknecht L, Jacob C, Strobel A, Kriegebaum C, Muller J, Zeng Y, Markert C, Escher A, Wendland J, Reif A, Mossner R, Gross C, Brocke B, Lesch KP (2007) Tryptophan hydroxylase-2 gene variation influences personality traits and disorders related to emotional dysregulation. Int J Neuropsychopharmacol 10:309-320.

Gutknecht L, Kriegebaum C, Waider J, Schmitt A, Lesch KP (2009) Spatio-temporal expression of tryptophan hydroxylase isoforms in murine and human brain: convergent data from Tph2 knockout mice. Eur Neuropsychopharmacol 19:266-282.

Gutknecht L, Waider J, Kraft S, Kriegebaum C, Holtmann B, Reif A, Schmitt A, Lesch KP (2008) Deficiency of brain 5-HT synthesis but serotonergic neuron formation in Tph2 knockout mice. J Neural Transm 115:1127-1132.

Gutknecht L, Waider J, Popp S, Araragi N, Sommerlandt F, Weber M, Göppner C, Colaço M, Post A, Wischmeyer E, Sommer C, Reif A, Palme R, Lesch K, (submitted) Brain serotonin deficiency promotes resilience to chronic stress via sex-specific adaptive mechanisms. submitted.

Haghighi F, Bach-Mizrachi H, Huang YY, Arango V, Shi S, Dwork AJ, Rosoklija G, Sheng HT, Morozova I, Ju J, Russo JJ, Mann JJ (2008) Genetic architecture of the human tryptophan hydroxylase 2 Gene: existence of neural isoforms and relevance for major depression. Mol Psychiatry 13:813-820.

Hale MW, Johnson PL, Westerman AM, Abrams JK, Shekhar A, Lowry CA (2010) Multiple anxiogenic drugs recruit a parvalbumin-containing subpopulation of GABAergic interneurons in the basolateral amygdala. Prog Neuropsychopharmacol Biol Psychiatry 34:1285-1293.

Harro J, Tonissaar M, Eller M, Kask A, Oreland L (2001) Chronic variable stress and partial 5-HT denervation by parachloroamphetamine treatment in the rat: effects on behavior and monoamine neurochemistry. Brain Res 899:227-239.

Harvey M, Shink E, Tremblay M, Gagne B, Raymond C, Labbe M, Walther DJ, Bader M, Barden N (2004) Support for the involvement of TPH2 gene in affective disorders. Mol Psychiatry 9:980-981.

Hensler JG (2006) Serotonergic modulation of the limbic system. Neurosci Biobehav Rev 30:203-214.

Hokfelt T, Broberger C, Xu ZQ, Sergeyev V, Ubink R, Diez M (2000) Neuropeptides--an overview. Neuropharmacology 39:1337-1356.

Holmes A (2008) Genetic variation in cortico-amygdala serotonin function and risk for stress-related disease. Neurosci Biobehav Rev 32:1293-1314.

Hornung JP (2003) The human raphe nuclei and the serotonergic system. J Chem Neuroanat 26:331-343.

Hurley MV, Scott DL, Rees J, Newham DJ (1997) Sensorimotor changes and functional performance in patients with knee osteoarthritis. Ann Rheum Dis 56:641-648.

Jacob CP, Muller J, Schmidt M, Hohenberger K, Gutknecht L, Reif A, Schmidtke A, Mossner R, Lesch KP (2005) Cluster B Personality Disorders are Associated with Allelic Variation of Monoamine Oxidase A Activity. Neuropsychopharmacology 30:1711-1718.

Jacobsen JP, Siesser WB, Sachs BD, Peterson S, Cools MJ, Setola V, Folgering JH, Flik G, Caron MG (2011) Deficient serotonin neurotransmission and depression-like serotonin biomarker alterations in tryptophan hydroxylase 2 (Tph2) loss-of-function mice. Mol Psychiatry.

Jinno S, Kosaka T (2006) Cellular architecture of the mouse hippocampus: a quantitative aspect of chemically defined GABAergic neurons with stereology. Neurosci Res 56:229-245.

Jinno S, Kosaka T (2010) Stereological estimation of numerical densities of glutamatergic principal neurons in the mouse hippocampus. Hippocampus 20:829-840.

Jungling K, Seidenbecher T, Sosulina L, Lesting J, Sangha S, Clark SD, Okamura N, Duangdao DM, Xu YL, Reinscheid RK, Pape HC (2008) Neuropeptide S-mediated control of fear expression and extinction: role of intercalated GABAergic neurons in the amygdala. Neuron 59:298-310.

Kalaska JF, Scott SH, Cisek P, Sergio LE (1997) Cortical control of reaching movements. Current Opinion in Neurobiology 7:849-859.

Keuker JI, Vollmann-Honsdorf GK, Fuchs E (2001) How to use the optical fractionator: an example based on the estimation of neurons in the hippocampal CA1 and CA3 regions of tree shrews. Brain Res Brain Res Protoc 7:211-221.

Kiyasova V, Fernandez SP, Laine J, Stankovski L, Muzerelle A, Doly S, Gaspar P (2011) A genetically defined morphologically and functionally unique subset of 5-HT neurons in the mouse raphe nuclei. J Neurosci 31:2756-2768.

Klausberger T (2009) GABAergic interneurons targeting dendrites of pyramidal cells in the CA1 area of the hippocampus. Eur J Neurosci 30:947-957.

Lawrence JJ (2008) Cholinergic control of GABA release: emerging parallels between neocortex and hippocampus. Trends in Neurosciences 31:317-327.

Lesch KP (2004) Gene-environment interaction and the genetics of depression. J Psychiatry Neurosci 29:174-184.

Lesch KP (2011) When the serotonin transporter gene meets adversity: the contribution of animal models to understanding epigenetic mechanisms in affective disorders and resilience. Curr Top Behav Neurosci 7:251-280.

Lesting J, Geiger M, Narayanan RT, Pape HC, Seidenbecher T (2011a) Impaired extinction of fear and maintained amygdala-hippocampal theta synchrony in a mouse model of temporal lobe epilepsy. Epilepsia 52:337-346.

Lesting J, Narayanan RT, Kluge C, Sangha S, Seidenbecher T, Pape HC (2011b) Patterns of coupled theta activity in amygdala-hippocampal-prefrontal cortical circuits during fear extinction. PLoS One 6:e21714.

Liu C, Maejima T, Wyler SC, Casadesus G, Herlitze S, Deneris ES (2010) Pet-1 is required across different stages of life to regulate serotonergic function. Nat Neurosci 13:1190-1198.

Liu N, Scott JG (1997) Inheritance of CYP6D1-mediated pyrethroid resistance in house fly (Diptera: Muscidae). J Econ Entomol 90:1478-1481.

Lopez VA, Detera-Wadleigh S, Cardona I, Kassem L, McMahon FJ (2007) Nested association between genetic variation in tryptophan hydroxylase II, bipolar affective disorder, and suicide attempts. Biol Psychiatry 61:181-186.

Lydiard RB (2003) The role of GABA in anxiety disorders. J Clin Psychiatry 64 Suppl 3:21-27.

Maier SF, Watkins LR (2005) Stressor controllability and learned helplessness: the roles of the dorsal raphe nucleus, serotonin, and corticotropin-releasing factor. Neurosci Biobehav Rev 29:829-841.

Mamounas LA, Mullen CA, O'Hearn E, Molliver ME (1991) Dual serotoninergic projections to forebrain in the rat: morphologically distinct 5-HT axon terminals exhibit differential vulnerability to neurotoxic amphetamine derivatives. J Comp Neurol 314:558-586.

McDonald AJ, Mascagni F (2001) Colocalization of calcium-binding proteins and GABA in neurons of the rat basolateral amygdala. Neuroscience 105:681-693.

McDonald AJ, Mascagni F (2007) Neuronal localization of 5-HT type 2A receptor immunoreactivity in the rat basolateral amygdala. Neuroscience 146:306-320.

McNaughton N, Corr PJ (2004) A two-dimensional neuropsychology of defense: fear/anxiety and defensive distance. Neuroscience & Biobehavioral Reviews 28:285-305.

Molliver ME (1987) Serotonergic neuronal systems: what their anatomic organization tells us about function. J Clin Psychopharmacol 7:3S-23S.

Mongeau R, Blier P, de Montigny C (1997) The serotonergic and noradrenergic systems of the hippocampus: their interactions and the effects of antidepressant treatments. Brain Res Brain Res Rev 23:145-195.

Mossner R, Walitza S, Geller F, Scherag A, Gutknecht L, Jacob C, Bogusch L, Remschmidt H, Simons M, Herpertz-Dahlmann B, Fleischhaker C, Schulz E, Warnke A, Hinney A, Wewetzer C, Lesch KP (2006) Transmission disequilibrium of polymorphic variants in the tryptophan hydroxylase-2 gene in children and adolescents with obsessive-compulsive disorder. Int J Neuropsychopharmacol 9:437-442.

Muller JF, Mascagni F, McDonald AJ (2005) Coupled networks of parvalbumin-immunoreactive interneurons in the rat basolateral amygdala. J Neurosci 25:7366-7376.

Nakamura K, Sugawara Y, Sawabe K, Ohashi A, Tsurui H, Xiu Y, Ohtsuji M, Lin QS, Nishimura H, Hasegawa H, Hirose S (2006) Late developmental stage-specific role of tryptophan hydroxylase 1 in brain serotonin levels. J Neurosci 26:530-534.

Navailles S, De Deurwaerdere P (2011) Presynaptic control of serotonin on striatal dopamine function. Psychopharmacology (Berl) 213:213-242.

Pape HC, Pare D (2010) Plastic synaptic networks of the amygdala for the acquisition, expression, and extinction of conditioned fear. Physiol Rev 90:419-463.

Porsolt RD, Le Pichon M, Jalfre M (1977) Depression: a new animal model sensitive to antidepressant treatments. Nature 266:730-732.

Post AM, Weyers P, Holzer P, Painsipp E, Pauli P, Wultsch T, Reif A, Lesch K-P (2011a) Gene-environment interaction influences anxiety-like behavior in ethologically based mouse models. Behavioural Brain Research 218:99-105.

Post AM, Wultsch T, Popp S, Painsipp E, Wetzstein H, Kittel-Schneider S, Sontag TA, Lesch K-P, Reif A (2011b) The COGITAT holeboard system as a valuable tool to assess learning, memory and activity in mice. Behavioural Brain Research 220:152-158.

Puig MV, Watakabe A, Ushimaru M, Yamamori T, Kawaguchi Y (2010) Serotonin modulates fast-spiking interneuron and synchronous activity in the rat prefrontal cortex through 5-HT1A and 5-HT2A receptors. J Neurosci 30:2211-2222.

Quinn JJ, Wied HM, Ma QD, Tinsley MR, Fanselow MS (2008) Dorsal hippocampus involvement in delay fear conditioning depends upon the strength of the tone-footshock association. Hippocampus 18:640-654.

Riad M, Zimmer L, Rbah L, Watkins KC, Hamon M, Descarries L (2004) Acute treatment with the antidepressant fluoxetine internalizes 5-HT1A autoreceptors and reduces the in vivo binding of the PET radioligand [18F]MPPF in the nucleus raphe dorsalis of rat. J Neurosci 24:5420-5426.

Riccio O, Potter G, Walzer C, Vallet P, Szabo G, Vutskits L, Kiss JZ, Dayer AG (2009) Excess of serotonin affects embryonic interneuron migration through activation of the serotonin receptor 6. Mol Psychiatry 14:280-290.

Rogers J, Ridley S, Chrispin P, Scotton H, Lloyd D (1997) Reliability of the next of kins' estimates of critically ill patients' quality of life. Anaesthesia 52:1137-1143.

Sadikot AF, Parent A (1990) The monoaminergic innervation of the amygdala in the squirrel monkey: an immunohistochemical study. Neuroscience 36:431-447.

Savelieva KV, Zhao S, Pogorelov VM, Rajan I, Yang Q, Cullinan E, Lanthorn TH (2008) Genetic disruption of both tryptophan hydroxylase genes dramatically reduces serotonin and affects behavior in models sensitive to antidepressants. PLoS One 3:e3301.

Scott MA, Li FX, Davids K (1997) Expertise and the regulation of gait in the approach phase of the long jump. J Sports Sci 15:597-605.

Seidenbecher T, Laxmi TR, Stork O, Pape H-C (2003) Amygdalar and Hippocampal Theta Rhythm Synchronization During Fear Memory Retrieval. Science 301:846-850.

Solomon PR, Nichols GL, Kiernan JM, 3rd, Kamer RS, Kaplan LJ (1980) Differential effects of lesions in medial and dorsal raphe of the rat: latent inhibition and septohippocampal serotonin levels. J Comp Physiol Psychol 94:145-154.

Soma M, Aizawa H, Ito Y, Maekawa M, Osumi N, Nakahira E, Okamoto H, Tanaka K, Yuasa S (2009) Development of the mouse amygdala as revealed by enhanced green fluorescent protein gene transfer by means of in utero electroporation. The Journal of Comparative Neurology 513:113-128.

Spampanato J, Polepalli J, Sah P (2011) Interneurons in the basolateral amygdala. Neuropharmacology 60:765-773.

Szabo GG, Holderith N, Gulyas AI, Freund TF, Hajos N (2010) Distinct synaptic properties of perisomatic inhibitory cell types and their different modulation by cholinergic receptor activation in the CA3 region of the mouse hippocampus. Eur J Neurosci 31:2234-2246.

Sziray N, Leveleki C, Levay G, Marko B, Harsing LG, Jr., Mikics E, Barsy B, Haller J (2007) Mechanisms underlying the long-term behavioral effects of traumatic experience in rats: the role of serotonin/noradrenaline balance and NMDA receptors. Brain Res Bull 71:376-385.

Thomas WJ, Laird JR, Bailey L, Hoopes TG, Hillhouse R, Scott D, Jones R, Virmani R, Carter AJ (1997) Experimental Results with the Multi-Link feminine Stent in a Porcine Model. J Invasive Cardiol 9:453-460.

Trudeau LE (2004) Glutamate co-transmission as an emerging concept in monoamine neuron function. J Psychiatry Neurosci 29:296-310.

Van Den Bogaert A, Sleegers K, De Zutter S, Heyrman L, Norrback KF, Adolfsson R, Van Broeckhoven C, Del-Favero J (2006) Association of brain-specific tryptophan hydroxylase, TPH2, with unipolar and bipolar disorder in a Northern Swedish, isolated population. Arch Gen Psychiatry 63:1103-1110.

Varga V, Losonczy A, Zemelman BV, Borhegyi Z, Nyiri G, Domonkos A, Hangya B, Holderith N, Magee JC, Freund TF (2009) Fast synaptic subcortical control of hippocampal circuits. Science 326:449-453.

Vitalis T, Cases O, Passemard S, Callebert J, Parnavelas JG (2007) Embryonic depletion of serotonin affects cortical development. Eur J Neurosci 26:331-344.

Waider J, Araragi N, Gutknecht L, Lesch KP (2011) Tryptophan hydroxylase-2 (TPH2) in disorders of cognitive control and emotion regulation: a perspective. Psychoneuroendocrinology 36:393-405.

Walitza S, Renner TJ, Dempfle A, Konrad K, Wewetzer C, Halbach A, Herpertz-Dahlmann B, Remschmidt H, Smidt J, Linder M, Flierl L, Knolker U, Friedel S, Schafer H, Gross C, Hebebrand J, Warnke A, Lesch KP (2005) Transmission disequilibrium of polymorphic variants in the tryptophan hydroxylase-2 gene in attention-deficit/hyperactivity disorder. Mol Psychiatry 10:1126-1132.

Walker DL, Miles LA, Davis M (2009) Selective participation of the bed nucleus of the stria terminalis and CRF in sustained anxiety-like versus phasic fear-like responses. Prog Neuropsychopharmacol Biol Psychiatry 33:1291-1308.

Walker DL, Toufexis DJ, Davis M (2003) Role of the bed nucleus of the stria terminalis versus the amygdala in fear, stress, and anxiety. Eur J Pharmacol 463:199-216.

West MJ (2001) Design based stereological methods for estimating the total number of objects in histological material. Folia morphologica 60:11-19.

Whitaker-Azmitia PM, Druse M, Walker P, Lauder JM (1996) Serotonin as a developmental signal. Behav Brain Res 73:19-29.

Wright DE, Seroogy KB, Lundgren KH, Davis BM, Jennes L (1995) Comparative localization of serotonin1A, 1C, and 2 receptor subtype mRNAs in rat brain. J Comp Neurol 351:357-373.

Zhang X, Beaulieu JM, Sotnikova TD, Gainetdinov RR, Caron MG (2004) Tryptophan hydroxylase-2 controls brain serotonin synthesis. Science 305:217.

Zill P, Baghai TC, Zwanzger P, Schule C, Eser D, Rupprecht R, Moller HJ, Bondy B, Ackenheil M (2004) SNP and haplotype analysis of a novel tryptophan hydroxylase isoform (TPH2) gene provide evidence for association with major depression. Mol Psychiatry 9:1030-1036.

Academic education

May 2008 until present

Doctoral thesis at the department of Psychiatry, Psychosomatics and Psychotherapy
University of Würzburg
Supervisor Prof. Dr. K.P. Lesch

October 2002 to April 2008

Graduate studies in Biology (Diploma) at the Julius-Maximilian-University of Würzburg
Focus on Neuroscience (main subject), Genetics and Microbiology

Diploma thesis at the Department of Psychiatry, Psychosomatics and Psychotherapy
University of Würzburg

"Spatial and temporal expression pattern of Tph1 and Tph2 in wild type mice and first characterization of a new mouse model for central serotonin deficiency"

Supervisor Prof. Dr. K.P. Lesch

April 2006 to September 2006

Visiting student at the faculty of Neuroscience University of Manchester
Lab rotation Prof. Dr. Ruth Itzhaki "Alzheimer Disease and HSV-1

8.2 List of publications

Gutknecht L, Kriegebaum C, Waider J, Schmitt A, Lesch KP (2009) Spatio-temporal expression of tryptophan hydroxylase isoforms in murine and human brain: convergent data from Tph2 knockout mice. Eur Neuropsychopharmacol 19:266-282.

Gutknecht L, Waider J, Kraft S, Kriegebaum C, Holtmann B, Reif A, Schmitt A, Lesch KP (2008) Deficiency of brain 5-HT synthesis but serotonergic neuron formation in Tph2 knockout mice. J Neural Transm 115:1127-1132.

Gutknecht L, Araragi N, Merker S, Waider J, Sommerlandt F, Mlinar B, Baccini G, Mayer U, Proft F, Hamon M, Schmitt A, Corradetti R, Lanfumey L, Lesch K (2012-a) Impacts of Brain serotonin deficiency following Tph2 inactivation on development and raphe neuron serotonergic specification. PlosOne under revision.

Gutknecht L, Waider J, Popp S, Araragi N, Sommerlandt F, Weber M, Göppner C, Colaço M, Post A, Wischmeyer E, Sommer C, Reif A, Palme R, Lesch K, (2012-b) Brain serotonin deficiency promotes resilience to chronic stress via sex-specific adaptive mechanisms. submitted

Waider J, Araragi N, Gutknecht L, Lesch KP (2011) Tryptophan hydroxylase-2 (TPH2) in disorders of cognitive control and emotion regulation: a perspective. Psychoneuroendocrinology 36:393-405.

Waider J, Proft F, Langlhofer G, Asan E, Lesch KP, Gutknecht L (2012) GABA concentration and interneuron subpopulations are differentially altered by brain serotonin deficiency in Tph2 knockout mice. Histochem Cell Biol under revision.

8.3 Affidavit

I hereby confirm that my thesis entitled “The effects of serotonin deficiency in mice: Focus on the GABAergic system” is the result of my own work. I did not receive any help or support from commercial consultants. All sources and / or materials are listed and specified in the thesis.

Furthermore, I confirm that this thesis has not yet been submitted as part of another examination process neither in identical nor in similar form.

Würzburg, 11.07.2012	
Place, Date	Signature

Hiermit erkläre ich an Eides statt die Dissertation “The effects of serotonin deficiency in mice: Focus on the GABAergic system” eigenständig, d.h.insbesondere selbststaändig und ohne die Hilfe eines kommerziellen Promotionsberaters, angefertigt und keine anderen als die von mir angegebenen Quellen und Hilfsmittel verwendet zu haben.

Ich erkläre außerdem, dass die Dissertation weder in gleicher noch in ähnlicher Form bereits in einem anderen Prüfungsverfahren vorgelegen hat.

Würzburg, 11.07.2012	
Ort, Datum	Unterschrift

8.4 Acknowledgment

I would like to thank Prof. Klaus-Peter Lesch for the opportunity to write the dissertation under his supervision. Beyond the excellent scientific education I was privileged to experience in the department and the scientific freedom I was granted, the stimulating but always cordially atmosphere in the department, which he has to take credit for, I have appreciate very much.

Furthermore, I would like to thank Lise, who taught me the secrets of science. Without her mice, enthusiasm, help and scientific knowledge this thesis would not have been realized.

I would like to thank Sören, Naozumi, Stephan, Markus, Angelika, Esther, Maria, Sarah N, Antonia, Lena and Sandy for the scientific collaboration.

Stephan, Sören and Judith for amusing “Doppelkopf” evenings

Of course my special thanks go to all TA`s in the department, without them good work would not have been possible in the lab. Especially I would like to thank Nicole for all the PCR work and for many chats away, Gabi for helping me out in the cell culture, Marion, who always had an ear for me in histology and Thomas for profound discussions and knowledge not only about soccer.

Finally yet importantly, I thank my family Jutta, Gerhard, Jan, Anne and especially Katja, Madlen Sophie and Carlotta Louisa for always reminding me that life is more than work but isn’t all beer and skittles

Dankeschön Euch allen !